POLITECNICO DI TORINO
Repository ISTITUZIONALE

Determining the extrinsic parameters of a network of Large-Volume Metrology sensors of different types

(Article begins on next page)

18 October 2022

Determining the extrinsic parameters of a network of Large-Volume Metrology sensors of different types

Domenico A. MAISANO[1,#] and Luca MASTROGIACOMO[2]

[1] domenico.maisano@polito.it, orcid.org/0000-0002-8154-4469, Politecnico di Torino, DIGEP (Dept. of Management and Production Engineering)

[2] luca.mastrogiacomo@polito.it, orcid.org/0000-0002-8454-5918, Politecnico di Torino, DIGEP (Dept. of Management and Production Engineering)

[#] Corresponding author

Abstract

Large-Volume Metrology (LVM) instruments – such as laser trackers, photogrammetric systems, rotary-laser automatic theodolites, etc. – generally include several *sensors*, which measure the distances and/or angles subtended by some *targets*. This measurements, combined with the spatial position/orientation of sensors (i.e., the so-called *extrinsic* parameters), can be used to locate targets in the measurement volume. Extrinsic parameters of sensors are generally determined through dedicated sensor calibration methods, which are based on repeated measurements of specific artefacts.

The combined use of multiple LVM instruments enables exploitation of available equipment but may require multiple instrument-dedicated sensor calibrations, which inevitably increase set-up time/cost.

This document presents a novel calibration method – called *global calibration* – which allows the extrinsic parameters of all sensors to be determined in a single process. The proposed method uses a special artefact – i.e., a hand-held *probe* with assorted types of targets and inertial sensors – and includes a data-acquisition stage, in which the probe is repositioned in different areas of the measurement volume, followed by a data-processing stage, in which an *ad hoc* mathematical/statistical model is used to determine the extrinsic parameters of sensors. Additionally, the proposed method includes the formulation of a system of linearized equations, which are weighed considering the uncertainty of input variables.

Keywords: Large-volume metrology, Distributed-sensor network, Extrinsic parameters, Multi-target probe, Artefact, Generalized Least Squares.

1. Introduction and literature review

Industrial applications in the field of *Large-Volume Metrology* (LVM) are typically concerned with the dimensional verification and assembly of large-sized mechanical components (e.g., aircraft/aerospace modules, automotive/commercial vehicles, large ships, wind turbines etc.). These applications generally require sub-millimetric levels of uncertainty and involve technologically advanced and expensive measuring instruments, which may require time consuming set-up operations [1-6].

Among the most common LVM instruments, laser trackers, laser radars, photogrammetric systems, and rotary-laser automatic theodolites (R-LATs) allow to accurately locate several targets. These instruments are usually equipped with *sensors* performing measurements of the *distances* and/or *angles* subtended by some *targets* within the measurement volume. LVM instruments can be classified into: (i) *centralized*, if sensors are grouped into a single (stand-alone) unit (e.g., a laser tracker or a photogrammetric bar that includes two/three rigidly connected cameras), or (ii) *distributed*, if sensors are freely positioned around the measurement volume (e.g., a set of R-LATs). Even though these instruments may differ in technology and metrological characteristics, they generally include a hand-held probe, which is equipped with some targets. An operator places the probe stylus in direct contact with the points of interest, i.e., on the surface of the measured object.

Several studies show that the combined use of LVM instruments of different nature can lead to a better exploitation of the available equipment and a systematic reduction in measurement uncertainty [7-9]. The underlying rationale is simple: in case several types of expensive LVM instruments were available in the same metrology laboratory or industrial workshop, it would be a waste to use them independently of each other (e.g., using a laser tracker for certain tasks only, a photogrammetric system for others, and so on). Instead, multiple LVM instruments could be used in conjunction, forming a LVM "macro-instrument" that includes a network of various sensors. The volume coverage and metrological performance of this macro-instrument are likely to be superior to those of the individual instruments [8].

Following this idea, a recently proposed mathematical/statistical approach, called "cooperative data fusion", combines the measurement data (i.e., distances and/or angles) from a network of LVM instruments/sensors in order to locate a target [10]. In this approach, measurement data by sensors of different types are fused and weighed according to the corresponding uncertainties, which means that more weight is given to the measurement data from more accurate sensors and *vice-versa*. Of course, the uncertainty in the resulting target location may vary depending on the amount of "more accurate" and "less accurate" sensors contributing to the measurement. It is interesting to observe that, in some practical cases, the more accurate sensors alone could not be sufficient to perform the target localization, making the contribution of the less accurate sensors indispensable.

Contribution [8] gives an emblematic example about a network of two sensors, i.e., (i) an accurate interferometric laser and (ii) a not-very-accurate photogrammetric camera, which separately would not be able to localize a target, but together would be able to do so. The same contribution contains another example concerning a network of (i) a scale-bar with three rigidly-connected photogrammetric cameras and (ii) a laser tracker, showing that the cooperative-data-fusion approach produces better results than using the individual instruments separately (i.e., competitive approach).

Moreover, a patent application of a modular and multi-target six-degrees-of-freedom (6DoF) probe for measurements with combinations of LVM instruments was filed [10-12]. Depending on the LVM instruments in use – the probe can be equipped with targets of different nature and integrated inertial sensors, which may contribute to the probe-location problem.

This document takes a step back from the probe-location problem, focusing on the (chronologically earlier) operation of sensor-network calibration. This operation is aimed at estimating a set of characteristic parameters, which can be distinguished into: (i) *extrinsic* parameters, i.e., parameters concerned with the spatial position and orientation of sensors (i.e., 3D coordinates and orientation angles), and (ii) *intrinsic* parameters, i.e., parameters concerned with other specific technical characteristics of sensors (e.g., the focal distance or lens distortion of photogrammetric sensors,

wavelength or air refractive index of interferometric sensors, etc.). Estimating these parameters accurately is critical to ensure a just as accurate probe location.

While the determination of intrinsic parameters can be performed from time to time, as long as the conditions of the environment and measurement instruments are relatively stable, the determination of extrinsic parameters should be performed whenever the sensor-network layout is changed. For example, considering that the focal distance (i.e., one of the intrinsic parameters) of a photogrammetric camera is relatively stable, it is not required to re-estimate this parameter very frequently [13].

In general, specific LVM instruments include dedicated sensor-calibration processes, which are based on repeated acquisitions, using specific artefacts [14-16].

Most often, data acquired are fitted by a mathematical model, based on the minimization of an error function. A range of general-purpose minimization algorithms can be used, such as those of Gauss-Newton and Levenberg-Marquardt [17].

When using combinations of different LVM instruments, it is needed to perform various instrument-dedicated calibration processes, which are based on the use of specific artefacts, acquisition procedures and optimization algorithms [1, 2, 6]. Since the sensors of a LVM instrument are generally located referring to a local Cartesian coordinate system, it is then imperative to align multiple local coordinate systems on a unique *absolute* coordinate system. Such *alignment* usually requires further measurements, using additional artefacts. Of particular interest is a recent novel technique that allows the alignment of multiple coordinate systems, without the use of calibrated artefacts [18].

Although calibration and alignment operations can be managed by relatively diffused commercial software packages, such as Spatial Analyzer®, Verisurf®, etc., the fact remains that they inevitably make set-up time/cost increase [19].

This document aims at developing a unique calibration method of a network of different types of sensors, which allows to determine their extrinsic parameters, in a single process and without the need for additional alignments. This calibration method will hereafter be referred to as "global" as it simultaneously involves all sensors of all

LVM measuring instruments. The same multi-target probe, which is used in the measurement phase to locate points of interest, can also be used in the network calibration phase, for data acquisition and to provide metrological traceability to the measurement unit of length.

Summarising, the proposed approach is based on five steps:

1. Introduction of suitable transformations to refer local Cartesian coordinate systems (e.g., those related to network sensors, probe, etc.) to a unique absolute coordinate system.

2. Construction of a system of equations relating to the measurements performed and the geometric characteristics of the artefacts in use;

3. Linearization of the above equations with respect to the unknown variables of the problem;

4. Weighing of the equations, based on the uncertainty contributions of the variables contained therein, through the *Multivariate Law of Propagation of Uncertainty* (MLPU) [20].

5. Solution of the system of equations through the *Generalized Least Squares* (GLS) method and determination of the unknown variables (with relevant uncertainties) [21].

The rest of the paper is divided into three sections. Sect. 2 describes the proposed methodology, formalizing the global-calibration problem from the mathematical/statistical point of view and illustrating the proposed solution. Sect. 3 contains a realistic example of data acquisition. Sect. 4 summarizes the main advantages of the proposed method, its limitations, and possible hints for future research. The Appendix section contains insights into a variety of issues, including hardware components adopted, transformations between coordinate systems, construction of matrices with sensor parameters, and mathematical formulation of equations.

2. Methodology

This section presents a global calibration procedure. Technical and mathematical details are discussed in the Appendix.

2.1 Hardware components

Let now consider a typical configuration consisting of: (i) a generic combination of LVM instruments with assorted network sensors, (ii) a hand-held probe with multiple targets and integrated inertial sensors (i.e., two-axis inclinometer and compass), and (iii) a number of acquisitions, in which the probe is repositioned several times within the measurement volume, collecting distance/angular measurements by the network sensors (with respect to probe targets) and angular measurement by the integrated inertial sensors.

As shown in the scheme in Fig. 1, LVM instruments are indicated with S_i (being $i = 1$, 2, …). The respective sensors of each i-th instrument are indicated with $s_{i,j}$ (being $j = 1$, 2, …). Each $i.j$-th sensor is able to measure the distances and/or angles subtended by some of the targets[1], i.e., those that are compatible with it and within the relevant communication range. Targets (T_k, being $k = 1$, 2, …) are rigidly mounted on a probe – which is described in detail in Sect. A.1.2 (in the Appendix). Several distance/angular measurements are performed during different acquisitions ($a = 1$, 2, ...), in which the probe is repositioned in different parts of the measurement volume.

The above configuration may include the use of additional artefacts such as bars or plates with different reference positions, on which to reposition the probe stylus during acquisitions [15].

Sect. A.1 (in the Appendix) provides an in-depth study of the main hardware components used for the global calibration procedure, illustrating their characteristic variables/parameters and the relevant scientific notation.

---

[1] A common assumption when dealing with LVM instruments is to consider targets and sensors as punctiform elements [2].
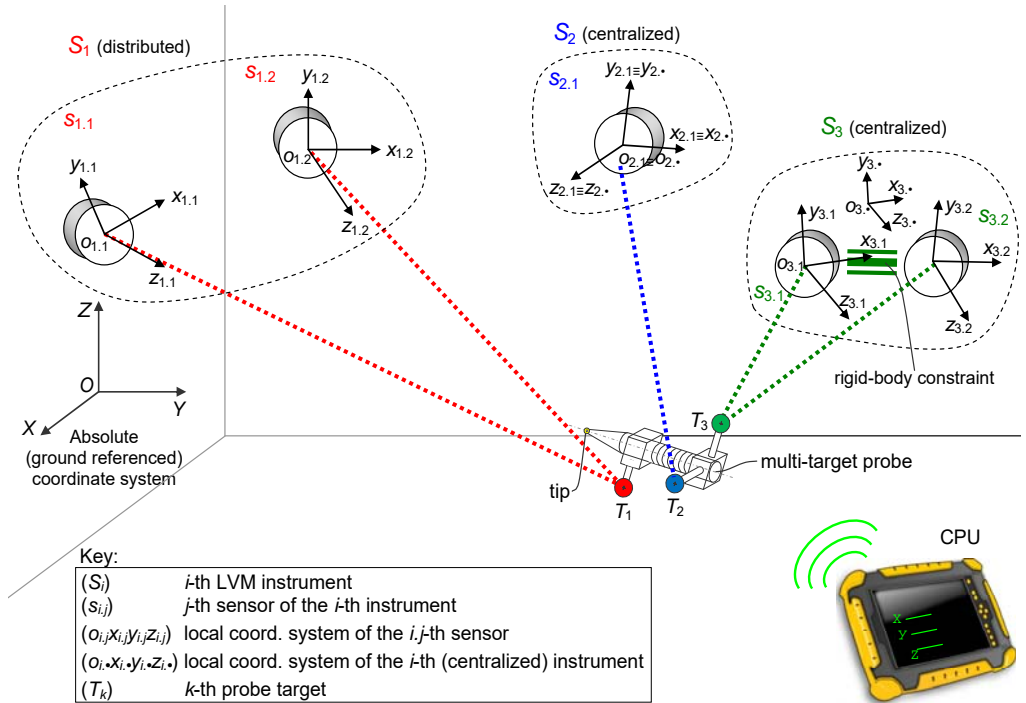
Fig. 1. Example of combination of three LVM instruments: S_1 **is a** *distributed* **instrument with two sensors** ($s_{1.1}$ **and** $s_{1.2}$)**, while** S_2 **and** S_3 **are two** *centralized* **instruments with one sensor** ($s_{2.1}$) **and two sensors** ($s_{3.1}$ **and** $s_{3.2}$) **respectively. The** *multi-target probe* **is equipped with three** *targets* (T_1**,** T_2 **and** T_3)**, which can be seen only by those** *sensors* **compatible with them (e.g.,** T_1 **can be seen by** $s_{1.1}$ **and** $s_{1.2}$**, not by** $s_{2.1}$**,** $s_{3.1}$ **and** $s_{3.2}$)**.**

Fig. 2 summarizes the variables/parameters of the global-calibration procedure and the coordinate systems in use. The total number of variables may depend on several features, such as:

- number of (centralized or distributed) LVM instruments and relevant sensors;
- characteristics of the probe in use (number and typology of targets);
- communication range of the sensors/targets in use;
- number of acquisitions.

We remark that all the (known or unknown) variables of the problem are dispersed and therefore associated with specific uncertainties. Since some of these variables can be correlated with each other, their variability can be expressed through variances and covariances. This aspect is developed in Sect. 2.3.
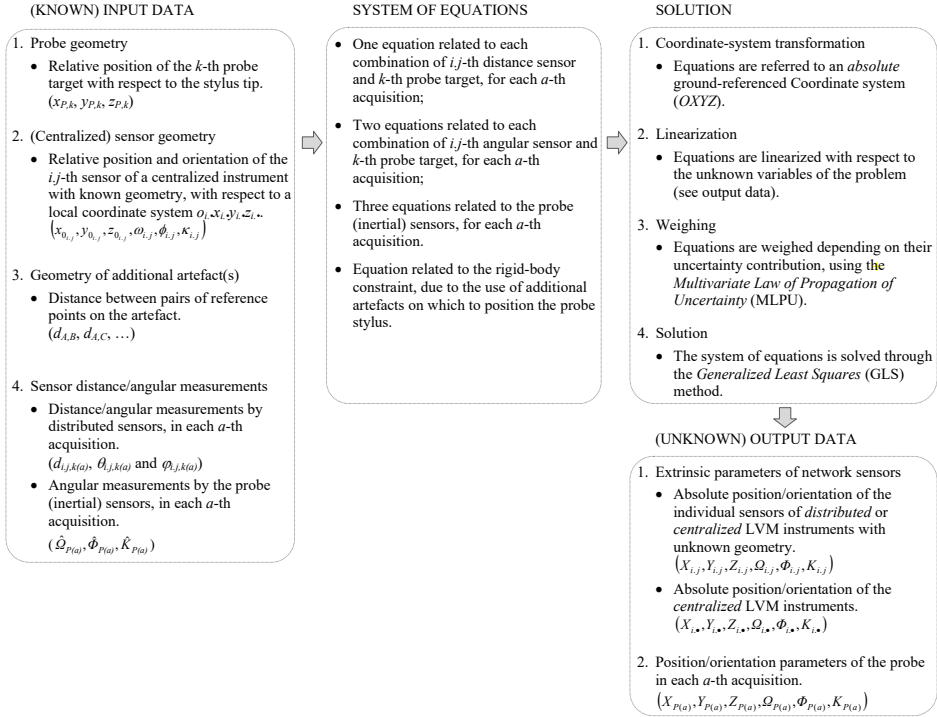
7

(KNOWN) INPUT DATA

1. Probe geometry
   - Relative position of the k-th probe target with respect to the stylus tip. $(x_{P,k}, y_{P,k}, z_{P,k})$

2. (Centralized) sensor geometry
   - Relative position and orientation of the $i.j$-th sensor of a centralized instrument with known geometry, with respect to a local coordinate system $o_i x_i y_i z_i$. $\left(x_{0_{i,j}}, y_{0_{i,j}}, z_{0_{i,j}}, \omega_{i,j}, \phi_{i,j}, \kappa_{i,j}\right)$

3. Geometry of additional artefact(s)
   - Distance between pairs of reference points on the artefact. $(d_{A,B}, d_{A,C}, \dots)$

4. Sensor distance/angular measurements
   - Distance/angular measurements by distributed sensors, in each a-th acquisition. $(d_{i,j,k(a)}, \theta_{i,j,k(a)}$ and $\varphi_{i,j,k(a)})$
   - Angular measurements by the probe (inertial) sensors, in each a-th acquisition. $(\hat{\Omega}_{P(a)}, \hat{\Phi}_{P(a)}, \hat{K}_{P(a)})$

SYSTEM OF EQUATIONS

- One equation related to each combination of $i.j$-th distance sensor and k-th probe target, for each a-th acquisition;
- Two equations related to each combination of $i.j$-th angular sensor and k-th probe target, for each a-th acquisition;
- Three equations related to the probe (inertial) sensors, for each a-th acquisition.
- Equation related to the rigid-body constraint, due to the use of additional artefacts on which to position the probe stylus.

SOLUTION

1. Coordinate-system transformation
   - Equations are referred to an *absolute* ground-referenced Coordinate system (*OXYZ*)

2. Linearization
   - Equations are linearized with respect to the unknown variables of the problem (see output data).

3. Weighing
   - Equations are weighed depending on their uncertainty contribution, using the *Multivariate Law of Propagation of Uncertainty* (MLPU).

4. Solution
   - The system of equations is solved through the *Generalized Least Squares* (GLS) method.

(UNKNOWN) OUTPUT DATA

1. Extrinsic parameters of network sensors
   - Absolute position/orientation of the individual sensors of *distributed* or *centralized* LVM instruments with unknown geometry. $\left(X_{i,j}, Y_{i,j}, Z_{i,j}, \Omega_{i,j}, \Phi_{i,j}, K_{i,j}\right)$
   - Absolute position/orientation of the *centralized* LVM instruments. $(X_{i,\bullet}, Y_{i,\bullet}, Z_{i,\bullet}, \Omega_{i,\bullet}, \Phi_{i,\bullet}, K_{i,\bullet})$

2. Position/orientation parameters of the probe in each a-th acquisition. $\left(X_{P(a)}, Y_{P(a)}, Z_{P(a)}, \Omega_{P(a)}, \Phi_{P(a)}, K_{P(a)}\right)$

Fig. 2. Scheme of the global-calibration procedure.

For practical reasons, the LVM instruments will be hereafter classified into two families:

Type-A instruments, which include distributed LVM instruments or centralized ones with unknown geometry (i.e., with unknown relative positions among sensors);

Type-B instruments, which includes centralized LVM instruments with known geometry (i.e., in terms of relative positions of the sensors that are rigidly connected to each other).

Additionally, the scheme in Fig. 1 represents an absolute ground-referenced coordinate system (*OXYZ*), with origin in a conventional point (for example, corresponding to one of the network sensors), Z axis vertical to ground plane, X axis pointing towards magnetic north, Y axis perpendicular to the two previous axes and oriented right-handedly. This choice was made to simplify the formulation of the equations related to the probe integrated (inertial) sensors.

For all hardware components used in the global calibration procedure, it is possible to define local Cartesian reference systems, which – thanks to appropriate roto-translation transformations – can be related to *OXYZ*. Sect. A.2 (in the Appendix) describes these transformations in detail.

2.2 Formulation of equations

Depending on the configuration of the LVM metrology instruments in use (e.g., sensor types, layout, etc.) and the acquisition procedure (e.g., number of acquisitions, use of artefacts, etc.), it is possible to formulate a system of equations including: (i) equations related to the distance measurements by network sensors, (ii) equations related to the angular measurements by network sensors, (iii) equations related to the probe's integrated sensors, and (iv) equations related to the additional artefact (if applicable).

Using the transformations between *local* and *global* coordinate systems (in Sect. A.2, in the Appendix), it is possible to formulate the equations, as functions of the (unknown) variables of the problem, which are contained in the following column vector:

$$
X = \begin{bmatrix} X^{type-A\ instr.} \\ X^{type-B\ instr.} \\ X^{probe} \end{bmatrix} = \begin{bmatrix} \begin{bmatrix} \vdots \\ X_{i.j}^{type-A\ instr.} \\ \vdots \end{bmatrix} \\ \begin{bmatrix} \vdots \\ X_{i.j}^{type-B\ instr.} \\ \vdots \end{bmatrix} \\ \vdots \\ \begin{bmatrix} \vdots \\ X_{(a)}^{probe} \\ \vdots \end{bmatrix} \end{bmatrix} = \begin{bmatrix} \begin{bmatrix} \vdots \\ \left[X_{i.j}, Y_{i.j}, Z_{i.j}, \Omega_{i.j}, \Phi_{i.j}, K_{i.j} \right]^T \\ \vdots \end{bmatrix} \\ \begin{bmatrix} \vdots \\ \left[X_{i.\bullet}, Y_{i.\bullet}, Z_{i.\bullet}, \Omega_{i.\bullet}, \Phi_{i.\bullet}, K_{i.\bullet} \right]^T \\ \vdots \end{bmatrix} \\ \begin{bmatrix} \vdots \\ \left[X_{P(a)}, Y_{P(a)}, Z_{P(a)}, \Omega_{P(a)}, \Phi_{P(a)}, K_{P(a)} \right]^T \\ \vdots \end{bmatrix} \end{bmatrix} . \quad (1)
$$

The variables contained in *X* are referenced to the absolute Cartesian coordinate system *OXYZ*; for details, please see Sect. A.1 (in the Appendix).

Next, equations can be linearised through a first order Taylor expansion with respect to the parameters contained in *X*. This linearization can be automated, e.g., using the Matlab's function "functionalDerivative" or other symbolic-calculation tools.

For a generic combination of LVM instruments with (i) various network sensors, (ii) a

probe with multiple targets and integrated sensors, and (iii) an additional calibrated artefact, the global-calibration problem can be formulated in compact form as:

$$
\mathbf{A} \cdot \mathbf{X} - \mathbf{B} = \begin{bmatrix} \mathbf{A}^{dist} \\ \mathbf{A}^{ang} \\ \mathbf{A}^{int} \\ \mathbf{A}^{art} \end{bmatrix} \cdot \mathbf{X} - \begin{bmatrix} \mathbf{B}^{dist} \\ \mathbf{B}^{ang} \\ \mathbf{B}^{int} \\ \mathbf{B}^{art} \end{bmatrix} = \mathbf{0} ,
\tag{2}
$$

where blocks $\mathbf{A}^{dist}$, $\mathbf{A}^{ang}$, $\mathbf{A}^{int}$, $\mathbf{A}^{art}$, $\mathbf{B}^{dist}$, $\mathbf{B}^{ang}$, $\mathbf{B}^{int}$ and $\mathbf{B}^{art}$ are defined as:

$$
\mathbf{A}^{dist} = \begin{bmatrix} \vdots \\ A^{dist}_{i.j,k(a)} \\ \vdots \end{bmatrix}, \ \mathbf{A}^{ang} = \begin{bmatrix} \vdots \\ A^{ang}_{i.j,k(a)} \\ \vdots \end{bmatrix}, \ \mathbf{A}^{int} = \begin{bmatrix} \vdots \\ A^{int}_{(a)} \\ \vdots \end{bmatrix}, \ \mathbf{A}^{art} = \begin{bmatrix} \vdots \\ A^{art}_{(a',a'')_c} \\ \vdots \end{bmatrix},
\tag{3}
$$

$$
\mathbf{B}^{dist} = \begin{bmatrix} \vdots \\ B^{dist}_{i.j,k(a)} \\ \vdots \end{bmatrix}, \ \mathbf{B}^{ang} = \begin{bmatrix} \vdots \\ B^{ang}_{i.j,k(a)} \\ \vdots \end{bmatrix}, \ \mathbf{B}^{int} = \begin{bmatrix} \vdots \\ B^{int}_{(a)} \\ \vdots \end{bmatrix}, \ \mathbf{B}^{art} = \begin{bmatrix} \vdots \\ B^{art}_{(a',a'')_c} \\ \vdots \end{bmatrix}.
$$

All equations of the system in Eq. 2 are linear(ized) and referenced to the absolute system *OXYZ*. The total number of unknown variables in the column vector $\mathbf{X}$ will depend on:

1. the configuration of the sensor network. In fact, there are six unknowns $(X_{i.j}, Y_{i.j}, Z_{i.j}, \Omega_{i.j}, \Phi_{i.j}, K_{i.j})$ for each sensor of a type-A instrument and six unknowns $(X_{i.\bullet}, Y_{i.\bullet}, Z_{i.\bullet}, \Omega_{i.\bullet}, \Phi_{i.\bullet}, K_{i.\bullet})$ for each type-B instrument, which is modelled as a single rigid-body with known geometry[2];

2. the number of acquisitions provided in the global-calibration procedure. For each *a*-th acquisition, the position and orientation of the probe $(X_{P(a)}, Y_{P(a)}, Z_{P(a)}, \omega_{P(a)}, \phi_{P(a)}, \kappa_{P(a)})$ are unknown.

---

[2] As explained in Sect. A.3.1 (in the Appendix), the unknowns related to *distance* sensors are only three, as the three orientation angles are arbitrary and can be omitted or replaced with arbitrary numerical values.

2.3 Weighting and solution

The equations may differently contribute to the uncertainty in the localization of network sensors and probe during acquisitions. The main uncertainty sources are:

- *Uncertainty in the local measurements by network sensors* ($\hat{d}_{i.j,k(a)}$, $\hat{\theta}_{i.j,k(a)}$ and $\hat{\varphi}_{i.j,k(a)}$), which depends on their metrological characteristics;

- *Uncertainty in the local measurements by the probe's integrated sensors* ($\hat{\Omega}_{P(a)}, \hat{\Phi}_{P(a)}, \hat{K}_{P(a)}$), which depends on their metrological characteristics;

- *Uncertainty in the relative position of the probe tip* (*P*) *with respect to probe targets* ($\hat{x}_k, \hat{y}_k$ and $\hat{z}_k$), which depends on the *ad hoc* geometric-calibration process of the probe;

- *Uncertainty in the relative position/orientation of the sensors of type-B instruments* ($\hat{x}_{0_{i.j}}, \hat{y}_{0_{i.j}}, \hat{z}_{0_{i.j}}, \hat{\omega}_{i.j}, \hat{\phi}_{i.j}, \hat{\kappa}_{i.j}$), which generally depends on the *ad hoc* calibration process of the (centralized) instrument;

- *Uncertainty in the mutual distances between pairs of reference points on the additional artefact* ($\hat{d}_{(a',a'')_c}$), which generally depends on the *ad hoc* geometric calibration of the additional artefact(s).

Since the system in Eq. 2 is *over-defined* (more equations than unknown parameters), there are several possible solution approaches [22, 23]. This system can be solved by applying the *Generalized Least Squares* (GLS) method, which gives greater weight to the contributions from equations that produce less uncertainty and *vice versa* [21]. This weighing allows the combination of data from measuring instruments/sensors with heterogeneous levels of uncertainty (e.g., less accurate sensors, such as low-cost photogrammetric cameras, and more accurate sensors, such as the interferometric distance sensor of a laser tracker).

The first step is to define a weight matrix (*W*) by applying the *Multivariate Law of Propagation of Uncertainty* (MLPU) to the system in Eq. 2, with reference to the parameters affected by uncertainty [24], which can be aggregated into a column vector

ξ. ξ can then be split into sub-vectors ξ^*, which group the akin input variables ("*" is a "wild-card" character that can be replaced with "probe", "type-B instr.", "add. artef.", "network sens.", "integr. Sens."):

$$\xi = \begin{bmatrix} \xi^{\,probe} \\ \xi^{\,type-B\ instr.} \\ \xi^{\,add.artef.} \\ \xi^{\,network\ sens.} \\ \xi^{\,integr.\ sens.} \end{bmatrix} = \begin{bmatrix} \left[\cdots \hat{x}_k, \hat{y}_k, \hat{z}_k \cdots\right]^T \\ \left[\cdots \hat{x}_{0_{i.j}}, \hat{y}_{0_{i.j}}, \hat{z}_{0_{i.j}}, \hat{\omega}_{i.j}, \hat{\phi}_{i.j}, \hat{\kappa}_{i.j} \cdots\right]^T \\ \left[\cdots \hat{d}_{(a',a'')_c} \cdots\right]^T \\ \left[\cdots \hat{d}_{i.j,k(a)}, \hat{\theta}_{i.j,k(a)}, \hat{\phi}_{i.j,k(a)} \cdots\right]^T \\ \left[\cdots \hat{\omega}_{P(a)}, \hat{\phi}_{P(a)}, \hat{\kappa}_{P(a)} \cdots\right]^T \end{bmatrix} . \tag{4}$$

Since the parameters into the sub-vectors $\xi^{\,probe}$, $\xi^{\,type-B\ instr.}$, and $\xi^{\,add.\ artef.}$ describe the geometric characteristics of the relevant hardware components, they require a preliminary estimation through *ad hoc* geometric calibration processes, for example using a coordinate-measuring machine (CMM). Consequently, these variables will contribute to metrological traceability with respect to the measurement unit of length.

Propagating the uncertainty of the equations in Eq. 2 with respect to the elements in ξ, W can be determined as:

$$W = \left[J \cdot \Sigma_\xi \cdot J^T\right]^{-1}, \tag{5}$$

being

J the Jacobian (block-diagonal) matrix with the partial derivatives of the elements in first members of Eq. 2 with respect to the elements in ξ;

Σ_ξ the covariance matrix of ξ.

An in-depth description of J and Σ_ξ is given in Sect. A.4 (in the Appendix).

The system of equations in Eq. 2 can then be solved through the GLS method [20, 21], obtaining a final estimate of X as:

$$\hat{X} = \left(A^T \cdot W \cdot A\right)^{-1} \cdot A^T \cdot W \cdot B . \tag{6}$$

An initial estimate of X is required to define some elements of the matrices A, B and W (demonstration omitted). This problem can be overcome applying Eq. 6

recursively: (i) setting (no-matter-what) initial values in $\hat{X}$, in order to determine the elements of matrices A, B and W, (ii) determining the unknown parameters in X, and (iii) iterating the solution using the result of the previous one as a new $\hat{X}$.

In general, the solution tends to converge after about five-ten iterations. When applying Eq. 6, it is generally recommended to replace the product between matrices $\left(A^T \cdot W \cdot A\right)^{-1} \cdot A^T \cdot W$ with the Moore-Penrose *pseudoinverse* of $A^T \cdot W \cdot A$, in order to avoid matrix conditioning problems [21].

2.4 Measurement uncertainty estimation

The mathematical/statistical model presented in Sects. 2.2 and 2.3 can also be used to determine the uncertainty in the estimate of X. Precisely, the covariance matrix Σ_X can be determined through the application of the *Multivariate Law of Propagation of Uncertainty* (MLPU) to the system of equations in Eq. 2, referring to the parameters affected by uncertainty in X [20, 24]:

$$\Sigma_X = \left(A^T \cdot W \cdot A\right)^{-1}. \tag{7}$$

The Σ_X matrix will depend on the characteristics of the sensor network (in terms of layout and metrological characteristics) and the geometric/metrological characteristics of the probe or additional artefact(s).

Sect. A.5 (in the Appendix) describes in detail Σ_X, showing the way to estimate the so-called *expanded* uncertainties related to the positions of the network sensors and the multi-target probe, during acquisitions.

3. Example of data acquisition

This section exemplifies the data acquisition stage, which includes three phases, described in the following sub-sections.

Phase 1: Spatial arrangement of network sensors

In the absence of design constraints, it is recommended that network sensors are spread around the measurement volume as homogeneously/uniformly as possible, i.e.

(i) avoiding concentrating them in certain areas, to the detriment of others, and (ii) trying to mix sensors of a different nature. These measures allow to cover the measurement volume in a relatively uniform way, avoiding that some areas are more "favoured" than others (e.g., maybe because they are covered by a greater amount of relatively accurate network sensors). A practical way to meet the above requirement is to position the sensors on the ceiling, according to a regular 2D grid, as described in [9].

For example, let consider a network of sensors, related to the three following LVM instruments (see Fig. 3):

(S_1) A photogrammetric system including three (distributed) photogrammetric cameras ($s_{1.1}$, $s_{1.2}$ and $s_{1.3}$);

(S_2) A laser tracker equipped with (i) an ADM (absolute distance meter) sensor ($s_{2.1}$), which provides distance measurements, and (ii) an angular sensor ($s_{2.2}$), which provides angular measurements ($s_{2.1} \equiv s_{2.2}$).

(S_3) An iSpace/iGPS system consisting of a single R-LAT sensor ($s_{3.1}$) [14-16].
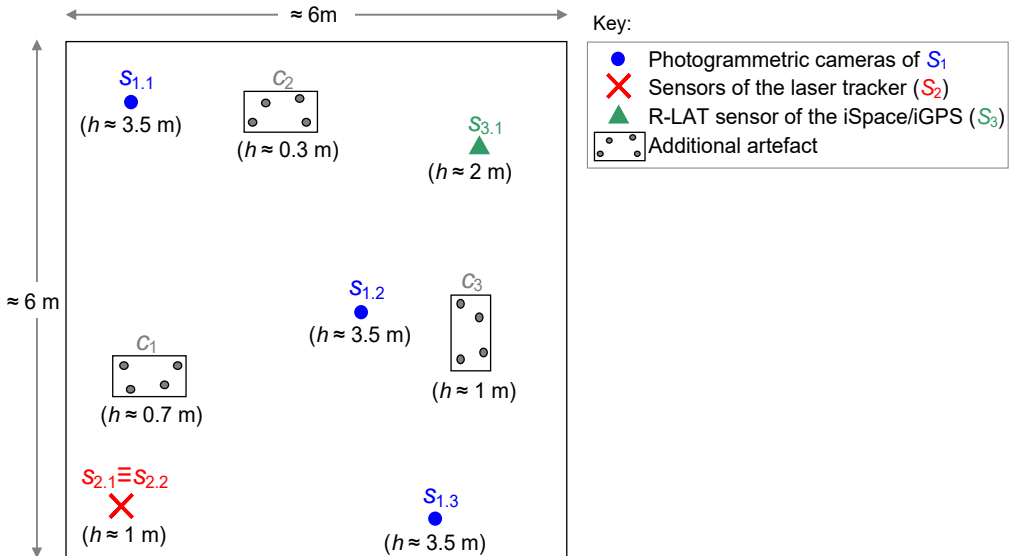
Fig. 3. Approximate layout of the sensor network and the additional artefact, during acquisitions (plant view). In brackets the approximate height of each device with respect to the floor level.

Phase 2: Multi-target probe set-up

The probe should have a relatively high number of targets, which are spaced as far apart as possible, but at the same time it should not be so bulky as to hinder its portability and handling [10, 12].

Returning to the previous example, we use a probe with the following characteristics (see Fig. 4):
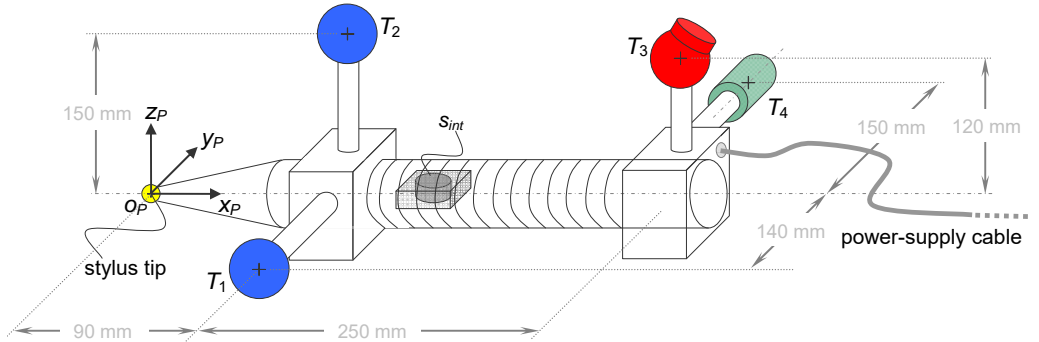

Fig. 4. Scheme of the probe adopted for data acquisition, including two reflective spherical markers (T_1 and T_2), a SMR (T_3), a R-LAT target (T_4), and two integrated inertial sensors (s_{int}).

- two reflective spherical markers (T_1 and T_2), which are visible from the three photogrammetric cameras ($s_{1.1}$, $s_{1.2}$ and $s_{1.3}$);
- a spherically mounted retroreflector (T_3), which is visible from the two laser-tracker sensors ($s_{2.1}$ and $s_{2.2}$);
- a R-LAT target (T_4), which is visible from the R-LAT sensor ($s_{3.1}$);
- a tip (P), which will be repositioned during acquisitions;
- two integrated (inertial) sensors (s_{int}, i.e., compass and two-axis inclinometer).

The probe geometry, in terms of relative positions between the targets and the tip, is determined in advance through an appropriate calibration process.

Phase 3: Data acquisition

During acquisitions, all network sensors should perform a certain number of (angular or distance) measurements with respect to relevant probe targets. To achieve this, the number of probe "repositionings" should be sufficient and they should be uniformly

distributed over the measuring volume. In general, for the *global calibration* procedure to provide relatively accurate results, the number of acquisitions must be redundant with respect to the strictly minimum number [20-22]. Acquisitions may also involve the use of additional artefact(s) on which to place the probe during the acquisitions. Knowledge of the geometry of the additional artefact(s) may help improve the accuracy of the solution provided, contributing to the metrological traceability with respect to the length unit of measurement [10, 12, 24].

Returning to the example, acquisitions are performed using a four-position (*A*, *B*, *C* and *D*) plate with known geometry. This artefact will be located in three different areas of the measurement volume (c_1, c_2 and c_3, as shown in Fig. 3) and the probe will be repositioned on the four reference positions, during acquisitions. The total number of acquisitions will therefore be twelve.

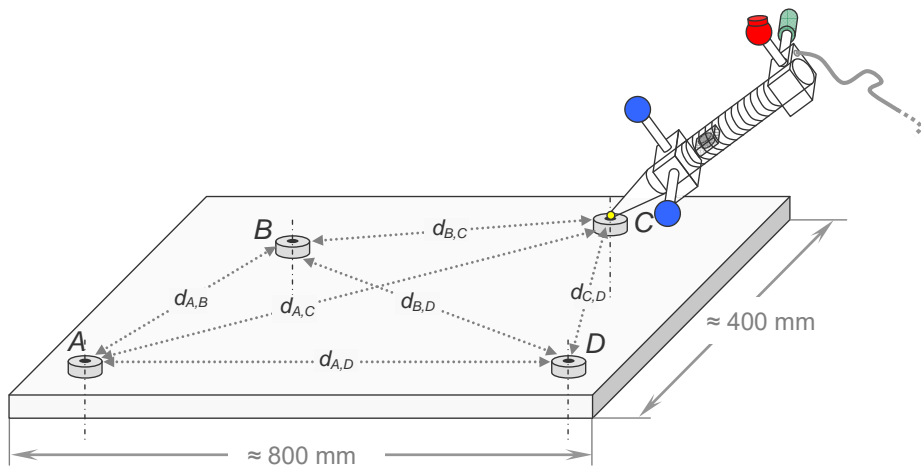Fig. 5 shows a qualitative representation of the artefact.

Fig. 5. Qualitative representation of the artefact exemplified. *A*, *B*, *C* and *D* **are four reference positions where to put the probe tip during acquisitions.**

3.1 Step-by-step acquisition

For a certain configuration of network sensors and probe targets, the number of acquisitions required for the global calibration procedure cannot be determined *a priori*, for (at least) three reasons:

- Since sensors have different coverage ranges, it is not easy to predict which probe target(s) will be covered in any acquisition. The possible presence of obstacles interposed between sensors and probe targets (e.g., operator, probe itself, measured object) may affect the sensor-target communication.

- It may happen that acquisitions are polarized on some sensors, "overlooking" others.

Therefore, there is a need for a real-time indication to assist the user during acquisitions. To fill this gap, an *ad hoc* software interface can be used. Precisely, each network sensor can be associated with a counter that records the number of measurements taken so far. For example, if a sensor performs two angular measurements and a single distance measurement with respect to some probe targets, the corresponding counter will be increased by three units. Each sensor can be associated with a parameter (m), which represents the number of measurements taken by the sensor of interest, with respect to one or more probe targets, up to that time. In general, the acquisition procedure continues as long as the following condition is met for each sensor:

$$m \geq t \cdot dof \ , \tag{8}$$

where:

dof (which stands for "degrees of freedom") is the number of unknown parameters for the sensor of interest, i.e., $dof = 6$ for angular or hybrid sensors (since they have three position and three orientation parameters) and $dof = 3$ for pure distance sensors (orientation is not influential);

t is a conventional threshold which should hopefully be greater than the unit, so that each sensor should take more measurements than the strictly necessary amount (dof) to determine the unknown parameters. In a later example, t will be set to 2.

For each network sensor, the quantity $\dfrac{m}{dof}$ can be shown to depict the acquisition-by-acquisition progress in data collection.

In practice, the operator is free to make acquisitions in the measurement volume, with some uniformity. Once he/she realizes that each network sensor has reached the quantity of required measurements (i.e., the target value of t is fulfilled), the acquisition procedure can be stopped and the mathematical/statistical procedure of global calibration launched (solving a linearized system of equations in Sects. 2.2 and 2.3).

Tab. 1 exemplifies a step-by-step evolution of acquisitions, placing the artefact in three positions (c_1 to c_3) within the measurement volume and – for each of them – repositioning the probe tip at points A, B, C and then D of the artefact (see Fig. 3 and Fig. 5). It can be noticed that network sensors gradually accumulate distance/angular measurements with respect to the probe targets, as the probe is repositioned during acquisitions. The threshold t has been conventionally set to 2. During acquisitions, not all network sensors are able to communicate with all probe targets compatible with them; see symbols "✘" in the columns "Angular/distance measurements".

The quantity of distance/angular measurements collected by each sensor by the end of the seventh acquisition (a_7) allows the condition in Eq. 8 to be met for any sensor. Indeed, at the end of the twelve acquisitions, a number of sensors have accumulated more than four times as many measurements as strictly needed ($m/dof \geq 4$). The gradual acquisition-by-acquisition results are also summarised in Fig. 6.

Acquisition	Ref. position	Network sensor	Typology	Target	Angular/distance measurements			Acquis. progress
					$\hat{d}_{i.j,k(a)}$	$\hat{\theta}_{i.j,k(a)}$	$\hat{\varphi}_{i.j,k(a)}$	(m/dof)
a_1	$c_1(A)$	$s_{1.1}$	angular	T_1	N/A	✔	✔	2/6 = 0.33
		idem	idem	T_2	N/A	✔	✔	4/6 = 0.67
		$s_{1.2}$	angular	T_1	N/A	✔	✔	2/6 = 0.33
		idem	idem	T_2	N/A	✔	✔	4/6 = 0.67
		$s_{1.3}$	angular	T_1	N/A	✘	✘	0/6 = 0.00
		idem	idem	T_2	N/A	✘	✘	0/6 = 0.00
		$s_{2.1}$	distance	T_3	✔	N/A	N/A	1/3 = 0.33
		$s_{2.2}$	angular	T_3	N/A	✔	✔	2/6 = 0.33
		$s_{3.1}$	angular	T_4	N/A	✔	✔	2/6 = 0.33
a_2	$c_1(B)$	$s_{1.1}$	angular	T_1	N/A	✔	✔	6/6 = 1.00
		idem	idem	T_2	N/A	✘	✘	6/6 = 1.00
		$s_{1.2}$	angular	T_1	N/A	✔	✔	6/6 = 1.00
		idem	idem	T_2	N/A	✔	✔	8/6 = 1.33
		$s_{1.3}$	angular	T_1	N/A	✔	✔	2/6 = 0.33
		idem	idem	T_2	N/A	✔	✔	4/6 = 0.67
		$s_{2.1}$	distance	T_3	✔	N/A	N/A	2/3 = 0.67
		$s_{2.2}$	angular	T_3	N/A	✔	✔	4/6 = 0.67
		$s_{3.1}$	angular	T_4	N/A	✔	✔	4/6 = 0.67

Acquisition	Ref. position	Network sensor	Typology	Target	$\hat{d}_{i.j.k(a)}$	$\hat{\theta}_{i.j.k(a)}$	$\hat{\varphi}_{i.j.k(a)}$	Acquis. progress (m/dof)
a_3	$c_1(C)$	$s_{1.1}$	angular	T_1	N/A	✗	✗	6/6 = 1.00
		idem	idem	T_2	N/A	✓	✓	8/6 = 1.33
		$s_{1.2}$	angular	T_1	N/A	✗	✗	8/6 = 1.33
		idem	idem	T_2	N/A	✓	✓	10/6 = 1.67
		$s_{1.3}$	angular	T_1	N/A	✗	✗	4/6 = 0.67
		idem	idem	T_2	N/A	✓	✓	6/6 = 1.00
		$s_{2.1}$	distance	T_3	✓	N/A	N/A	3/3 = 1.00
		$s_{2.2}$	angular	T_3	N/A	✓	✓	6/6 = 1.00
		$s_{3.1}$	angular	T_4	N/A	✓	✓	6/6 = 1.00
a_4	$c_1(D)$	$s_{1.1}$	angular	T_1	N/A	✓	✓	10/6 = 1.67
		idem	idem	T_2	N/A	✓	✓	12/6 = 2.00
		$s_{1.2}$	angular	T_1	N/A	✓	✓	12/6 = 2.00
		idem	idem	T_2	N/A	✓	✓	14/6 = 2.33
		$s_{1.3}$	angular	T_1	N/A	✓	✓	8/6 = 1.33
		idem	idem	T_2	N/A	✓	✓	10/6 = 1.67
		$s_{2.1}$	distance	T_3	✗	N/A	N/A	3/3 = 1.00
		$s_{2.2}$	angular	T_3	N/A	✗	✗	6/6 = 1.00
		$s_{3.1}$	angular	T_4	N/A	✓	✓	8/6 = 1.33
a_5	$c_2(A)$	$s_{1.1}$	angular	T_1	N/A	✓	✓	14/6 = 2.33
		idem	idem	T_2	N/A	✓	✓	16/6 = 2.67
		$s_{1.2}$	angular	T_1	N/A	✓	✓	16/6 = 2.67
		idem	idem	T_2	N/A	✓	✓	18/6 = 3.00
		$s_{1.3}$	angular	T_1	N/A	✓	✓	12/6 = 2.00
		idem	idem	T_2	N/A	✓	✓	14/6 = 2.33
		$s_{2.1}$	distance	T_3	✓	N/A	N/A	4/3 = 1.33
		$s_{2.2}$	angular	T_3	N/A	✓	✓	8/6 = 1.33
		$s_{3.1}$	angular	T_4	N/A	✗	✗	8/6 = 1.33
a_6	$c_2(B)$	$s_{1.1}$	angular	T_1	N/A	✗	✗	16/6 = 2.67
		idem	idem	T_2	N/A	✗	✗	16/6 = 2.67
		$s_{1.2}$	angular	T_1	N/A	✗	✗	18/6 = 3.00
		idem	idem	T_2	N/A	✗	✗	18/6 = 3.00
		$s_{1.3}$	angular	T_1	N/A	✗	✗	14/6 = 2.33
		idem	idem	T_2	N/A	✗	✗	14/6 = 2.33
		$s_{2.1}$	distance	T_3	✓	N/A	N/A	5/3 = 1.67
		$s_{2.2}$	angular	T_3	N/A	✓	✓	10/6 = 1.67
		$s_{3.1}$	angular	T_4	N/A	✓	✓	10/6 = 1.67
a_7	$c_2(C)$	$s_{1.1}$	angular	T_1	N/A	✓	✓	18/6 = 3.00
		idem	idem	T_2	N/A	✗	✗	18/6 = 3.00
		$s_{1.2}$	angular	T_1	N/A	✓	✓	20/6 = 3.33
		idem	idem	T_2	N/A	✗	✗	20/6 = 3.33
		$s_{1.3}$	angular	T_1	N/A	✓	✓	16/6 = 2.67
		idem	idem	T_2	N/A	✓	✓	18/6 = 3.00
		$s_{2.1}$	distance	T_3	✓	N/A	N/A	6/3 = 2.00
		$s_{2.2}$	angular	T_3	N/A	✓	✓	12/6 = 2.00
		$s_{3.1}$	angular	T_4	N/A	✓	✓	12/6 = 2.00
a_8	$c_2(D)$	$s_{1.1}$	angular	T_1	N/A	✓	✓	20/6 = 3.33
		idem	idem	T_2	N/A	✓	✓	22/6 = 3.67
		$s_{1.2}$	angular	T_1	N/A	✓	✓	22/6 = 3.67
		idem	idem	T_2	N/A	✓	✓	24/6 = 4.00
		$s_{1.3}$	angular	T_1	N/A	✗	✗	18/6 = 3.00
		idem	idem	T_2	N/A	✗	✗	18/6 = 3.00
		$s_{2.1}$	distance	T_3	✓	N/A	N/A	7/3 = 2.33
		$s_{2.2}$	angular	T_3	N/A	✓	✓	14/6 = 2.33
		$s_{3.1}$	angular	T_4	N/A	✓	✓	14/6 = 2.33
a_9	$c_3(A)$	$s_{1.1}$	angular	T_1	N/A	✓	✓	24/6 = 4.00
		idem	idem	T_2	N/A	✓	✓	26/6 = 4.33
		$s_{1.2}$	angular	T_1	N/A	✓	✓	26/6 = 4.33
		idem	idem	T_2	N/A	✓	✓	28/6 = 4.67

Acquisition	Ref. position	Network sensor	Typology	Target	Angular/distance measurements $\hat{d}_{i.j,k(a)}$	$\hat{\theta}_{i.j,k(a)}$	$\hat{\varphi}_{i.j,k(a)}$	Acquis. progress (m/dof)
		$s_{1.3}$	angular	T_1	N/A	✔	✔	20/6 = 3.33
		idem	idem	T_2	N/A	✔	✔	22/6 = 3.67
		$s_{2.1}$	distance	T_3	✔	N/A	N/A	8/3 = 2.67
		$s_{2.2}$	angular	T_3	N/A	✔	✔	16/6 = 2.67
		$s_{3.1}$	angular	T_4	N/A	✘	✘	14/6 = 2.33
a_{10}	$c_3(B)$	$s_{1.1}$	angular	T_1	N/A	✔	✔	28/6 = 4.67
		idem	idem	T_2	N/A	✔	✔	30/6 = 5.00
		$s_{1.2}$	angular	T_1	N/A	✔	✔	30/6 = 5.00
		idem	idem	T_2	N/A	✔	✔	32/6 = 5.33
		$s_{1.3}$	angular	T_1	N/A	✔	✔	24/6 = 4.00
		idem	idem	T_2	N/A	✔	✔	26/6 = 4.33
		$s_{2.1}$	distance	T_3	✘	N/A	N/A	8/3 = 2.67
		$s_{2.2}$	angular	T_3	N/A	✘	✘	16/6 = 2.67
		$s_{3.1}$	angular	T_4	N/A	✔	✔	16/6 = 2.67
a_{11}	$c_3(C)$	$s_{1.1}$	angular	T_1	N/A	✘	✘	32/6 = 5.33
		idem	idem	T_2	N/A	✘	✘	34/6 = 5.67
		$s_{1.2}$	angular	T_1	N/A	✘	✘	32/6 = 5.33
		idem	idem	T_2	N/A	✘	✘	32/6 = 5.33
		$s_{1.3}$	angular	T_1	N/A	✘	✘	26/6 = 4.33
		idem	idem	T_2	N/A	✘	✘	26/6 = 4.33
		$s_{2.1}$	distance	T_3	✔	N/A	N/A	9/3 = 3.00
		$s_{2.2}$	angular	T_3	N/A	✔	✔	18/6 = 3.00
		$s_{3.1}$	angular	T_4	N/A	✔	✔	18/6 = 3.00
a_{12}	$c_3(D)$	$s_{1.1}$	angular	T_1	N/A	✔	✔	36/6 = 6.00
		idem	idem	T_2	N/A	✔	✔	38/6 = 6.33
		$s_{1.2}$	angular	T_1	N/A	✔	✔	34/6 = 5.67
		idem	idem	T_2	N/A	✘	✘	34/6 = 5.67
		$s_{1.3}$	angular	T_1	N/A	✔	✔	28/6 = 4.67
		idem	idem	T_2	N/A	✘	✘	28/6 = 4.67
		$s_{2.1}$	distance	T_3	✔	N/A	N/A	10/3 = 3.33
		$s_{2.2}$	angular	T_3	N/A	✔	✔	20/6 = 3.33
		$s_{3.1}$	angular	T_4	N/A	✔	✔	20/6 = 3.33

Tab. 1. Gradual data acquisition related to the sensors exemplified in Fig. 3. The symbols "✔" and "✘" indicate respectively the measurements taken and not taken in a certain acquisition. The last column (*m/dof*) indicates the degree of progress of acquisitions, from the point of view of any single sensor; cells highlighted in green indicate that the condition in Eq. 8 is met, having set *t*=2.
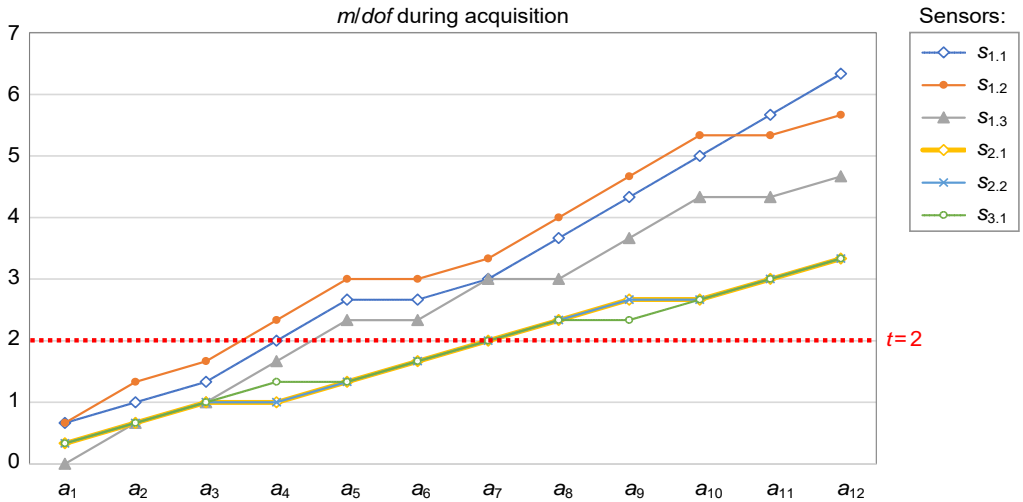
Fig. 6. Graph summarising the gradual acquisition data in Tab. 1. The vertical axis shows the degree of progress (*m/dof*) of acquisitions (*a*₁ to *a*₁₂) from the point of view of any single sensor.

4. Conclusions

This section discusses (i) the implications, (ii) limitations and (iii) future development of this research.

4.1 Implications

The global calibration is *versatile*, since it can be adapted to a variety of LVM instruments with sensors performing distance/angular measurements with respect to targets. It is relatively *quick*, since it allows to locate the network sensors through a single acquisition process, using a special artefact (i.e., multi-target hand-held probe) and avoiding multiple instrument-dedicated calibration processes or alignment of local coordinate systems. It is *computationally light*, as it is based on a system of linearized equations, and *statistically rigorous*, as the equations are weighted with respect to the uncertainty contributions of the input variables. It also makes it possible to determine the uncertainty related to the position/orientation of network sensors.

This method can be categorized as *bundle adjustment* as it allows to "adjust" the location of network sensors and probe, through several acquisitions in which the probe is repositioned in the measurement volume [17, 25].

The proposed global calibration can encourage the combined use of LVM instruments of different nature, assuming they are already available in a metrology laboratory or industrial workshop. This combined use is nowadays relatively limited, due to the lack of suitable (hardware and software) tools and support methods. Apart from the use of a multi-target probe [12], the proposed method may include additional artefacts where to reposition the probe during acquisitions; the use of these artefacts may help improve the metrological traceability with respect to the length and the accuracy in the sensor network location. At the time of writing, an *ad hoc* software application to guide the user through the various global-calibration stages (i.e., input of probe/sensor geometric data, sensor measurement acquisition, formulation and solution of the system of equations) is under development.

Due to the originality/innovativeness content and the industrial applicability, the global calibration procedure was patented [26].

4.2 Limitations

The proposed method allows to estimate the *extrinsic* parameters of the network sensors, assuming that the *intrinsic* ones are already known. Intrinsic parameters can be determined from time to time, as long as the conditions of the measurement environment are relatively stable.

In addition, appropriate *ad hoc* calibration processes need to be performed in advance, so as to determine the information concerned with the geometry of the probe, the additional artefact, and the type-B instruments in use. At the time of writing, these processes are carried out through a series of dimensional measurements using a DEA Global Image coordinate measuring machine (CMM), with a Maximum Permissible Error (MPE) of 3 μm. These measurements are partly automated thanks to a dedicated routine in the CMM's software application (PC-DMIS).

The proposed solution technique requires initial estimates of the X unknown variables, i.e., a rough estimate of the sensor network layout and the position/orientation of the probe during acquisitions. However, it was experimentally verified that the

mathematical/statistical model converges relatively quickly to the correct solution, even with relatively rough initial estimates [7, 8].

Finally, the fact that the greater effectiveness of *cooperative* versus *competitive* localization methods was quantitatively assessed [9] represents partial evidence of the greater effectiveness of the proposed global calibration (cooperative approach) compared to the combination of traditional instrument-dedicated calibration processes (competitive approach). Nevertheless, the present study did not provide direct evidence of this, which will be the object of future research.

4.3 Future development

We plan to perform an experimental factorial plan to study the link between the effectiveness of the sensor-network calibration and some potentially influential factors, such as:

- number of acquisitions;
- use of additional artefact(s) besides the multi-target probe;
- accuracy in the geometric calibration of the probe and artefacts.

This study, apart from allowing a quantitative assessment of the effectiveness of global calibration may also support the design of appropriate acquisitions, according to the desired accuracy in establishing the extrinsic parameters of the network sensors. [16].

In addition, we plan to make a structured comparison of the results obtained by applying the global calibration procedure and those obtained through multiple instrument-dedicated calibration processes, from different viewpoints (e.g., accuracy in the location of the sensor network, time and simplicity of execution, etc.).

Acknowledgements

Short CVs

Domenico A. Maisano received the M.Sc. degree (*cum laude*) in "Mechanical Engineering" in 2003 and the Ph.D. degree in "Industrial Production Systems Engineering" in 2008, from Politecnico di Torino, Italy. He is currently Associate Professor of "Quality Engineering" and "Quality Management" at Politecnico di Torino – Dept. of Management and Production Engineering (DIGEP). His major research interests are Quality Engineering/Management, Large Volume Metrology, Performance Indicators and Scientometrics. He is (co-)author of 6 books, around 200 publications on international journals, book chapters, conference proceedings, and 3 patent applications.

Luca Mastrogiacomo received the M.Sc. degree (*cum laude*) in "Mathematical Engineering" in 2006 and the Ph.D. degree in "Industrial Production Systems Engineering" in 2009, from Politecnico di Torino, Italy. He is currently Associate Professor of "Production Systems" and "Quality Management" at Politecnico di Torino – Dept. of Management and Production Engineering (DIGEP). His major research interests are Industrial Metrology, Collaborative Robotics and Quality Management. He is (co-)author of 3 books, around 150 publications on international journals, book chapters, conference proceedings, and 3 patent applications.

References

[1] Peggs, G.N., Maropoulos, P.G., Hughes, E.B., Forbes, A.B., Robson, S., Ziebart, M., Muralikrishnan, B. (2009) Recent developments in large-scale dimensional metrology. Proceedings of the Institution of Mechanical Engineers, Part B: Journal of Engineering Manufacture, 223(6): 571-595.

[2] Franceschini, F., Galetto, M., Maisano, D., Mastrogiacomo, L., Pralio, B. (2011) Distributed Large-Scale Dimensional Metrology, Springer, London.

[3] Maropoulos, P.G., Muelaner, J.E., Summers, M.D., Martin, O.C. (2014). A new paradigm in large-scale assembly—research priorities in measurement assisted assembly. The International Journal of Advanced Manufacturing Technology, 70(1-4): 621-633.

[4] Franceschini, F., Maisano, D. (2014). The evolution of large-scale dimensional metrology from the perspective of scientific articles and patents. The International Journal of Advanced Manufacturing Technology, 70(5-8), 887-909.

[5] Franceschini, F., Galetto, M., Maisano, D., Mastrogiacomo, L. (2014b). Large-scale dimensional metrology (LSDM): from tapes and theodolites to multi-sensor systems. International Journal of Precision Engineering and Manufacturing, 15(8), 1739-1758.

[6] Schmitt, R.H., Peterek, M., Morse, E., Knapp, W., Galetto, M., Härtig, F., ... & Estler, W.T. (2016). Advances in large-scale metrology–review and future trends. CIRP Annals, 65(2), 643-665.

[7] Galetto, M., Mastrogiacomo, L., Maisano, D., Franceschini, F. (2015). Cooperative fusion of distributed multi-sensor LVM (Large Volume Metrology) systems, CIRP Annals - Manufacturing Technology, 64(1): 483-486.

[8] Franceschini, F., Galetto, M., Maisano, D., Mastrogiacomo, L. (2016). Combining multiple Large Volume Metrology systems: Competitive versus cooperative data fusion. Precision Engineering, 43: 514-524.

[9] Maisano, D., Mastrogiacomo, L. (2016). A new methodology to design multi-sensor networks for distributed large-volume metrology systems based on triangulation. Precision Engineering, 43, 105-118.

[10] Maisano, D., Mastrogiacomo, L. (2018). A novel multi-target modular probe for multiple large-volume metrology systems. Precision Engineering, 52: 30-54.

[11] Maisano, D.A., Mastrogiacomo, L., Galetto, M., Franceschini, F. (2016) Dispositivo tastatore e procedimento di localizzazione di un dispositivo tastatore per la misura di oggetti di grandi dimensioni, Italian patent application, serial number 102016000107650, filed on 25/10/2016 and granted on 13/03/2019.

[12] Maisano, D., Mastrogiacomo, L. (2019). A new mathematical model to localize a multi-target modular probe for large volume-metrology applications. In Advanced Mathematical and Computational Tools in Metrology and Testing XI (pp. 235-240), World Scientific, DOI: 10.1142/9789813274303_0022.

[13] Svoboda, T., Martinec, D., Pajdla, T. (2005). A convenient multicamera self-calibration for virtual environments. PRESENCE: teleoperators and virtual environments, 14(4): 407-422.

[14] ARCSecond (2002) Indoor GPS technology for Metrology. White Paper 071502, ARCSecond, [accessed: 09-06-2021] Dulles, http://www.cs.columbia.edu/~drexel/CandExam/ARCSecond_Indoor_GPS_Techn ology_for_Metrology.pdf

[15] Maisano, D.A., Jamshidi, J., Franceschini, F., Maropoulos, P.G., Mastrogiacomo, L., Mileham, A., Owen, G. (2008). Indoor GPS: system functionality and initial performance evaluation. International Journal of Manufacturing Research, 3(3), 335-349.

[16] Wang, Z., Mastrogiacomo, L., Franceschini, F., Maropoulos, P. (2011). Experimental comparison of dynamic tracking performance of iGPS and laser tracker. The international journal of advanced manufacturing technology, 56(1): 205-213.

[17] Lourakis, M.I.A., Argyros, A.A. (2009). SBA: a software package for generic sparse bundle adjustment. ACM Transactions on Mathematical Software, 36(1): 1-30.

[18] Pfeifer, T., Montavon, B., Peterek, M., Hughes, B. (2019). Artifact-free coordinate registration of heterogeneous Large-Scale Metrology systems. CIRP Annals, 68(1), 503-506.

[19] Ferri, C., Mastrogiacomo, L., Faraway, J. (2010) Sources of variability in the set-up of an Indoor GPS. International Journal of Computer Integrated Manufacturing, 23(6): 487-499.

[20] Ross, S.M. (2009). Introduction to probability and statistics for engineers and scientists. Academic Press.

[21] Kariya, T., Kurata, H. (2004) Generalized least squares, John Wiley & Sons, New York.

[22] Wolberg, J. (2005) Data Analysis Using the Method of Least Squares: Extracting the Most Information from Experiments. Springer. ISBN 3-540-25674-1.

[23] Franceschini, F., Maisano, D., Mastrogiacomo, L. (2014a). Cooperative diagnostics for distributed large-scale dimensional metrology systems based on triangulation. Proceedings of the Institution of Mechanical Engineers, Part B: Journal of Engineering Manufacture, 228(4): 479-492.

[24] Hall, B.D. (2004). On the propagation of uncertainty in complex-valued quantities. Metrologia, 41(3): 173.

[25] Triggs, B., McLauchlan, P. F., Hartley, R. I., Fitzgibbon, A. W. (1999). Bundle adjustment—a modern synthesis. In International workshop on vision algorithms (pp. 298-372). Springer, Berlin, Heidelberg.

[26] Mastrogiacomo, L., Maisano, D.A. (2019) Metodo per la taratura di un sistema di misura LVM ibrido, Italian patent application, serial number 102019000006619, filed on 07/05/2019 and granted on 15/03/2021.

[27] Maisano, D.A., Mastrogiacomo, L., Galetto, M., Franceschini, F. (2016) Dispositivo tastatore e procedimento di localizzazione di un dispositivo tastatore per la misura di oggetti di grandi dimensioni, Italian patent application, serial number 102016000107650, filed on 25/10/2016 and granted on 13/03/2019.

[28] Franceschini, F., Galetto, M., Maisano, D.A., Mastrogiacomo, L., Bai, O. (2017) Feeler device, marker for a feeler device and system for taking photogrammetric measurements of objects, International Patent Application No. WO2017122112A1, WIPO (Patent Cooperation Treaty), International publication date: 20/07/2017.

Appendix

A.1 In-depth study of hardware components

This section goes deeper into the description of the hardware components used in the global-calibration procedure – i.e., network sensors, multi-target probe, and artefacts – illustrating their characteristic variables/parameters.

A.1.1 Network sensors

The distances and angles, which are measured by the $i.j$-th sensor with respect to the k-th target during the a-th acquisition, are respectively $d_{i.j,k(a)}$, $\theta_{i.j,k(a)}$ and $\varphi_{i.j,k(a)}$; Fig. A.1 represents them, referring to a *local* coordinate system $(o_{i.j}x_{i.j}y_{i.j}z_{i.j})$ that is centred into the $i.j$-th sensor itself.

Network sensors are positioned freely around the measurement volume and therefore have unknown position/orientation and relevant uncertainties. Considering a ground-referenced absolute Cartesian coordinate system – $OXYZ$, with vertical Z axis and X axis along the direction of the north-magnetic pole, and origin (O) in a conventional point within the measurement volume – we can define the origin of the local reference system of each sensor as $o_{i.j} = (X_{0_{i.j}}, Y_{0_{i.j}}, Z_{0_{i.j}})$ and the corresponding axis rotation parameters as $\Omega_{i.j}, \Phi_{i.j}, K_{i.j}$.
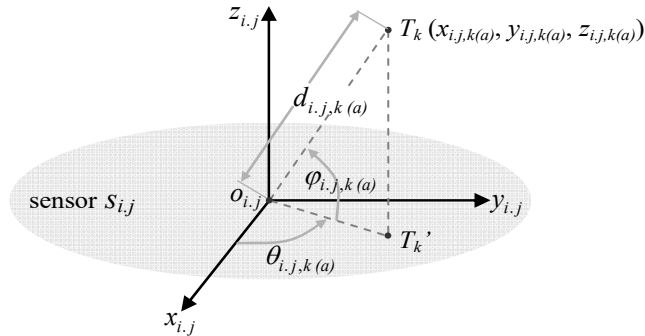
Fig. A.1. For a generic $i.j$-th sensor ($s_{i.j}$) and a generic a-th acquisition, a line joining the k-th probe target (T_k) and the origin ($o_{i.j}$) of the local coordinate system $o_{i.j}x_{i.j}y_{i.j}z_{i.j}$ subtends a distance ($d_{i.j,k(a)}$) and two angles – i.e., $\theta_{i.j,k(a)}$ (azimuth) and $\varphi_{i.j,k(a)}$ (elevation).

For *centralized* LVM instruments, sensors are rigidly constrained between each other. In other words, each of these instruments can be seen as a rigid body (with six degrees of freedom in the three-dimensional space), with another local coordinate system $o_{i.}x_{i.}y_{i.}z_{i.}$, which is centred at a conventional point and a conventional axis orientation. The position $(x_{i.j}, y_{i.j}, z_{i.j})$ and orientation $(\Omega_{i.j}, \Phi_{i.j}, K_{i.j})$ of a generic sensor, and the relevant uncertainties in this other local coordinate system may be determined through an initial calibration process of the centralized-instrument's geometry, e.g., performing a direct measurement using a Coordinate Measuring Machine (CMM) or other indirect measurement methods.

The (unknown) coordinates of $o_{i.}$ in *OXYZ* are $X_{0_{i.}}, Y_{0_{i.}}, Z_{0_{i.}}$, while the (unknown) rotation parameters of the $x_{i.}$, $y_{i.}$ and $z_{i.}$ axes, with respect to *OXYZ*, are respectively $\Omega_{i.}, \Phi_{i.}, K_{i.}$.

A.1.2 Multi-target probe

The probe that is used for acquisitions can be interpreted as a rigid body, whose target positions (T_k) are known with a corresponding uncertainty. We conventionally define a local coordinate system, $o_P x_P y_P z_P$, which is centred in the stylus tip and has a conventional orientation. The probe can be located in three-dimensional space, determining the parameters $X_{P(a)}, Y_{P(a)}, Z_{P(a)}, \Omega_{P(a)}, \Phi_{P(a)}, K_{P(a)}$, which correspond to the stylus position and the spatial orientation of the probe itself. Subscript "*P*" stands for "probe" or "point" (*P*), while subscript "*a*" indicates that the position/orientation of the probe may change from acquisition to acquisition.

The probe is equipped with integrated inertial sensors, which can (roughly) measure the probe orientation angles: $\hat{\Omega}_{P(a)}, \hat{\Phi}_{P(a)}, \hat{K}_{P(a)}$. We note that these angular measurements are direct estimates of the unknown angles $\Omega_{P(a)}, \Phi_{P(a)}, K_{P(a)}$, and do not depend on the combinations of *i.j*-th network sensors and *k*-th targets involved in the acquisitions; for this reason, they will be denoted by the subscript "*a*" only. For simplicity, it is also assumed that $\hat{\Omega}_{P(a)}, \hat{\Phi}_{P(a)}, \hat{K}_{P(a)}$ are directly referred to the absolute coordinate system *OXYZ*.

Focusing on the probe targets, their configuration can be varied depending on the LVM instruments/sensors used. Once this configuration has been defined, it is possible to determine the relative positions of each k-th target with respect to a local reference system. As already said, it can be assumed that the origin (o_P) of the probe's local reference system ($o_P x_P y_P z_P$) is in the stylus tip; the relative coordinates of each k-th target ($x_{P,k}$, $y_{P,k}$, $z_{P,k}$) and the relevant uncertainty may be determined through an initial *ad hoc* geometric calibration of the probe parts, e.g., using a CMM.

Fig. A.2 shows some pictures of a prototype probe developed at Politecnico di Torino – DIGEP. The structural "endoskeleton" and the target modules are in carbon fibre, since this material is relatively rigid, lightweight and with a small thermal-expansion coefficient. A special coupling system guarantees a relatively quick, precise, and repeatable insertion of the target modules into a primary module [27].
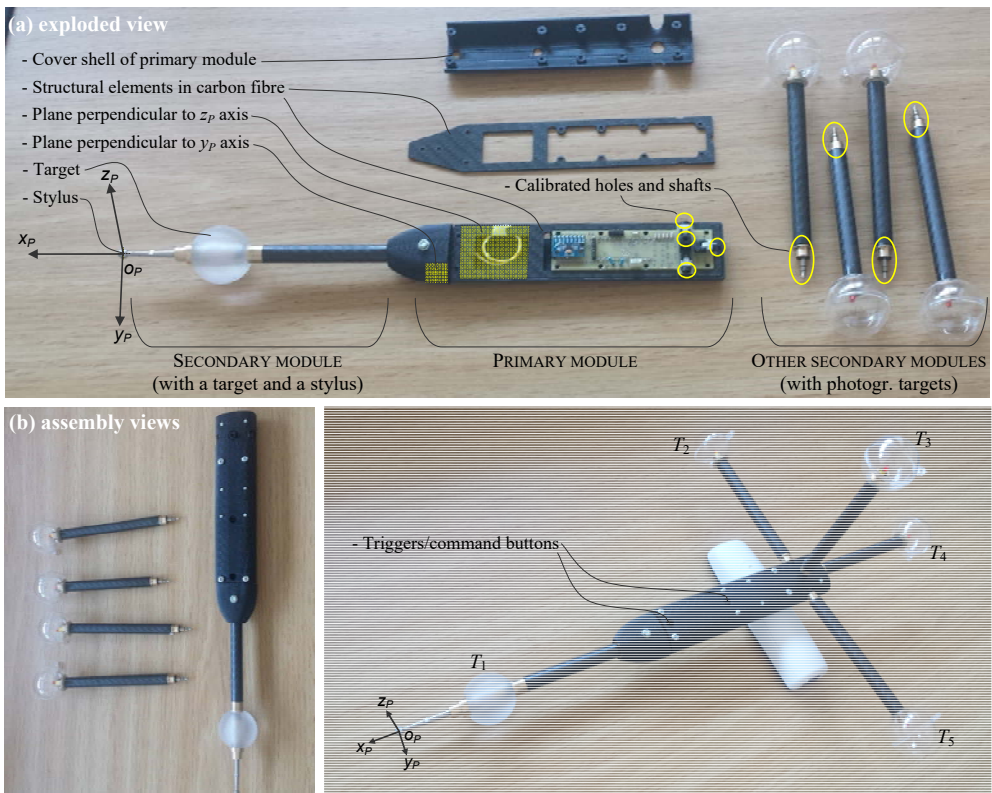
Fig. A.2. Prototype probe developed at Politecnico di Torino – DIGEP. In this case, the probe mounts five active photogrammetric targets (T_1 to T_5) [27, 28].

A.1.3 Additional artefacts

The proposed procedure may also include additional artefacts, such as bars or plates with different reference positions, on which to reposition the probe stylus during acquisitions. For example, Fig. 5 illustrates a plate with four mounts (*A*, *B*, *C* and *D*) with mutual distances $d_{A,B}$, $d_{A,C}$, etc., which can be measured through an *ad hoc* geometric calibration process (e.g., using a CMM).

Sect. A.3.4 will show that this information can be used in the global calibration problem, contributing to the metrological traceability to the unit of measurement of length [10, 12, 24].

A.2 Transformations between Cartesian coordinate systems

This section is divided into three subsections, dedicated respectively to (i) network sensors, (ii) multi-target probe and (iii) probe's integrated sensors.

A.2.1 Local coordinate system related to network sensors

The single LVM instruments can be centralized or distributed: in the former case, sensors are rigidly connected to each other, while in the latter, they are not.

Focusing the attention on the generic sensor ($s_{i,j}$) of an *i*-th type-A LVM instrument, it will be positioned freely around the measurement volume and will have a local coordinate system ($o_{i,j}x_{i,j}y_{i,j}z_{i,j}$), which is roto-translated with respect to the absolute one (*OXYZ*). The position/orientation of $o_{i,j}x_{i,j}y_{i,j}z_{i,j}$ with respect to *OXYZ* (i.e., $X_{0_{i,j}}, Y_{0_{i,j}}, Z_{0_{i,j}}$, $\Omega_{i,j}$, $\Phi_{i,j}$, $K_{i,j}$) is defined by the so-called *extrinsic* parameter, which represent (part of) the unknowns of the problem.

A general transformation between a local and the absolute coordinate system is:

$$
\begin{bmatrix} X \\ Y \\ Z \end{bmatrix} = \boldsymbol{R_{i,j}} \cdot \begin{bmatrix} x_{i,j} \\ y_{i,j} \\ z_{i,j} \end{bmatrix} + \begin{bmatrix} X_{0_{i,j}} \\ Y_{0_{i,j}} \\ Z_{0_{i,j}} \end{bmatrix}.
\tag{9}
$$

$\boldsymbol{R_{i,j}}$ is a 3x3 matrix, whose elements are functions of three rotation angles $\Omega_{i,j}$, $\Phi_{i,j}$, $K_{i,j}$:

$$\boldsymbol{R_{i.j}} = \begin{bmatrix} \cos\Phi_{i.j}\cos K_{i.j} & -\cos\Phi_{i.j}\sin K_{i.j} & \sin\Phi_{i.j} \\ \cos\Omega_{i.j}\sin K_{i.j} + \sin\Omega_{i.j}\sin\Phi_{i.j}\cos K_{i.j} & \cos\Omega_{i.j}\cos K_{i.j} - \sin\Omega_{i.j}\sin\Phi_{i.j}\sin K_{i.j} & -\sin\Omega_{i.j}\cos\Phi_{i.j} \\ \sin\Omega_{i.j}\sin K_{i.j} - \cos\Omega_{i.j}\sin\Phi_{i.j}\cos K_{i.j} & \sin\Omega_{i.j}\cos K_{i.j} + \cos\Omega_{i.j}\sin\Phi_{i.j}\sin K_{i.j} & \cos\Omega_{i.j}\cos\Phi_{i.j} \end{bmatrix}, \quad (10)$$

where $\Omega_{i.j}$ represents a counterclockwise rotation around the $x_{i.j}$ axis; $\Phi_{i.j}$ represents a counterclockwise rotation around the new $y_{i.j}$ axis, which was rotated by $\Omega_{i.j}$; $K_{i.j}$ represents a counterclockwise rotation around the new $z_{i.j}$ axis, which was rotated by $\Omega_{i.j}$ and then $\Phi_{i.j}$; for details, see [23]. $\left[X_{0_{i.j}}, Y_{0_{i.j}}, Z_{0_{i.j}}\right]^T$ are the coordinates of the origin of $o_{i.j}x_{i.j}y_{i.j}z_{i.j}$ in the absolute coordinate system $OXYZ$.

The coordinates of a generic point $(x_{i.j}, y_{i.j}, z_{i.j})$, referring to the local Cartesian reference system $(o_{i.j}x_{i.j}y_{i.j}z_{i.j})$, can be expressed as a function of the coordinates (X, Y, Z) in the absolute coordinate reference system. Reversing Eq. 9 and considering that $\boldsymbol{R_{i.j}^{-1}} = \boldsymbol{R_{i.j}^{T}}$ ($\boldsymbol{R_{i.j}}$ is orthonormal), we obtain:

$$\begin{bmatrix} x_{i.j} \\ y_{i.j} \\ z_{i.j} \end{bmatrix} = \boldsymbol{R_{i.j}^{-1}} \left\{ \begin{bmatrix} X \\ Y \\ Z \end{bmatrix} - \begin{bmatrix} X_{0_{i.j}} \\ Y_{0_{i.j}} \\ Z_{0_{i.j}} \end{bmatrix} \right\} = \boldsymbol{R_{i.j}^{T}} \left\{ \begin{bmatrix} X \\ Y \\ Z \end{bmatrix} - \begin{bmatrix} X_{0_{i.j}} \\ Y_{0_{i.j}} \\ Z_{0_{i.j}} \end{bmatrix} \right\}. \quad (11)$$

Assuming that (i) the point $(x_{i.j}, y_{i.j}, z_{i.j})$ corresponds to the position of the k-th probe target in the a-th acquisition $(x_{i.j,k(a)}, y_{i.j,k(a)}, z_{i.j,k(a)})$ and (ii) the absolute position of that point in the absolute system $OXYZ$ $(X_{k(a)}, Y_{k(a)}, Z_{k(a)})$, the equation notation will be slightly modified into:

$$\begin{bmatrix} x_{i.j,k(a)} \\ y_{i.j,k(a)} \\ z_{i.j,k(a)} \end{bmatrix} = \boldsymbol{R_{i.j}^{T}} \left\{ \begin{bmatrix} X_{k(a)} \\ Y_{k(a)} \\ Z_{k(a)} \end{bmatrix} - \begin{bmatrix} X_{0_{i.j}} \\ Y_{0_{i.j}} \\ Z_{0_{i.j}} \end{bmatrix} \right\}. \quad (12)$$

For each type-B LVM instrument, we can define another local Cartesian coordinate system $(o_{i.}x_{i.}y_{i.}z_{i.})$ with origin $(o_{i.})$ in a conventional point that is integral with the instrument itself and conventional coordinate axes; for example, $o_{i.}x_{i.}y_{i.}z_{i.}$ may coincide with the coordinate system of one of the sensors. The subscript "$i.$" indicates that the coordinate system is related to the whole i-th (centralized) LVM instrument,

irrespective of the single *i.j*-th sensor that is rigidly connected to it. Similarly to Eq. 9, a general transformation between this local system and the absolute one is:

$$
\begin{bmatrix} X \\ Y \\ Z \end{bmatrix} = \boldsymbol{R}_{i.\bullet} \cdot \begin{bmatrix} x_{i.\bullet} \\ y_{i.\bullet} \\ z_{i.\bullet} \end{bmatrix} + \begin{bmatrix} X_{0_{i.\bullet}} \\ Y_{0_{i.\bullet}} \\ Z_{0_{i.\bullet}} \end{bmatrix}.
\tag{13}
$$

where $\boldsymbol{R}_{i.\bullet}$ is a 3x3 rotation matrix depicting the orientation of the *i*-th centralized instrument with respect to the absolute system (*OXYZ*). The elements of this matrix are expressed as functions of three (unknown) rotation angles $\Omega_{i.\bullet}$, $\Phi_{i.\bullet}$, $K_{i.\bullet}$, which are analogous to $\Omega_{i.j}$, $\Phi_{i.j}$, $K_{i.j}$ (in Eq. 10) but are related to the axes $x_{i.\bullet}$, $y_{i.\bullet}$, $z_{i.\bullet}$, instead of $x_{i.j}$, $y_{i.j}$, $z_{i.j}$. $[X_{0_{i.\bullet}}, Y_{0_{i.\bullet}}, Z_{0_{i.\bullet}}]^T$ are the (unknown) coordinates of the origin of $o_{i.\bullet}x_{i.\bullet}y_{i.\bullet}z_{i.\bullet}$, in *OXYZ*.

Each *i.j*-th sensor of the centralized instrument has a local reference system $o_{i.j}x_{i.j}y_{i.j}z_{i.j}$. A general transformation between the coordinates of a generic point referred to this system and those referred to $o_{i.\bullet}x_{i.\bullet}y_{i.\bullet}z_{i.\bullet}$ is:

$$
\begin{bmatrix} x_{i.\bullet} \\ y_{i.\bullet} \\ z_{i.\bullet} \end{bmatrix} = \boldsymbol{r}_{i.j} \cdot \begin{bmatrix} x_{i.j} \\ y_{i.j} \\ z_{i.j} \end{bmatrix} + \begin{bmatrix} x_{0_{i.j}} \\ y_{0_{i.j}} \\ z_{0_{i.j}} \end{bmatrix}.
\tag{14}
$$

where

$\boldsymbol{r}_{i.j}$ is a 3x3 rotation matrix depicting the orientation of the *i.j*-th sensor with respect to $o_{i.\bullet}x_{i.\bullet}y_{i.\bullet}z_{i.\bullet}$. The elements of this matrix are functions of three (unknown) rotation parameters $\omega_{i.j}$, $\phi_{i.j}$, $\kappa_{i.j}$ related to the axes $x_{i.j}$, $y_{i.j}$ and $z_{i.j}$. $[x_{0_{i.\bullet}}, y_{0_{i.\bullet}}, z_{0_{i.\bullet}}]^T$ are the (unknown) coordinates of the origin of $o_{i.j}x_{i.j}y_{i.j}z_{i.j}$, in the other local coordinate system $o_{i.\bullet}x_{i.\bullet}y_{i.\bullet}z_{i.\bullet}$. If the geometry of the centralized LVM instrument is known, the parameters $x_{0_{i.j}}, y_{0_{i.j}}, z_{0_{i.j}}$, $\omega_{i.j}$, $\phi_{i.j}$, $\kappa_{i.j}$ can be determined; e.g., they can be deduced from the technical specifications of the centralized instrument or can be determined experimentally by a geometric calibration of the instrument itself.

A generic point with coordinates $[x_{i.j}, y_{i.j}, z_{i.j}]^T$ can be referred to *OXYZ*, by combining Eqs. 13 and 14:

$$\begin{bmatrix} X \\ Y \\ Z \end{bmatrix} = \boldsymbol{R_{i.\bullet}} \cdot \left\{ \boldsymbol{r_{i.j}} \cdot \left[\begin{bmatrix} x_{i.j} \\ y_{i.j} \\ z_{i.j} \end{bmatrix} + \begin{bmatrix} x_{0_{i.j}} \\ y_{0_{i.j}} \\ z_{0_{i.j}} \end{bmatrix} \right] \right\} + \begin{bmatrix} X_{0_{i.\bullet}} \\ Y_{0_{i.\bullet}} \\ Z_{0_{i.\bullet}} \end{bmatrix} . \tag{15}$$

Reversing Eq. 15 and considering that $\boldsymbol{R_{i.\bullet}}$ and $\boldsymbol{r_{i.j}}$ are orthonormal (therefore $\boldsymbol{R_{i.\bullet}^{-1}} = \boldsymbol{R_{i.\bullet}^{T}}$ and $\boldsymbol{r_{i.j}^{-1}} = \boldsymbol{r_{i.j}^{T}}$) we obtain:

$$\begin{bmatrix} x_{i.j} \\ y_{i.j} \\ z_{i.j} \end{bmatrix} = \boldsymbol{r_{i.j}^{T}} \cdot \left(\boldsymbol{R_{i.\bullet}^{T}} \cdot \left\{ \begin{bmatrix} X \\ Y \\ Z \end{bmatrix} - \begin{bmatrix} X_{0_{i.\bullet}} \\ Y_{0_{i.\bullet}} \\ Z_{0_{i.\bullet}} \end{bmatrix} \right\} - \begin{bmatrix} x_{0_{i.j}} \\ y_{0_{i.j}} \\ z_{0_{i.j}} \end{bmatrix} \right) . \tag{16}$$

Assuming that (i) the point $(x_{i.j}, y_{i.j}, z_{i.j})$ corresponds to the position of the k-th probe target in the a-th acquisition $(x_{i.j,k(a)}, y_{i.j,k(a)}, z_{i.j,k(a)})$ and (ii) we should determine the position of that point in $OXYZ$, the notation of Eq. 16 can be slightly modified into:

$$\begin{bmatrix} x_{i.j,k(a)} \\ y_{i.j,k(a)} \\ z_{i.j,k(a)} \end{bmatrix} = \boldsymbol{r_{i.j}^{T}} \cdot \left(\boldsymbol{R_{i.\bullet}^{T}} \cdot \left\{ \begin{bmatrix} X_{k(a)} \\ Y_{k(a)} \\ Z_{k(a)} \end{bmatrix} - \begin{bmatrix} X_{0_{i.\bullet}} \\ Y_{0_{i.\bullet}} \\ Z_{0_{i.\bullet}} \end{bmatrix} \right\} - \begin{bmatrix} x_{0_{i.j}} \\ y_{0_{i.j}} \\ z_{0_{i.j}} \end{bmatrix} \right) . \tag{17}$$

Regarding the centralized LVM instruments with *unknown* geometry (i.e., type-A instruments), the relevant sensors can be treated as if they were positioned independently of each other, i.e., in the same manner of the sensors of distributed LVM instruments (see Eqs. 11 and 12). Of course, this simplification will lead to lose part of the information that can be used for solving the problem.

A.2.2 Local coordinate system related to the probe tip

Focusing on a probe that is equipped with various targets (T_1, T_2, ..., T_k, ...), the absolute position of the k-th target in the a-th acquisition is $T_{k(a)} = [X_{k(a)}, Y_{k(a)}, Z_{k(a)}]^T$. The probe has a local coordinate system $o_P x_P y_P z_P$, which is centred with respect to the probe tip ($o_P = P$, see Fig. A.3). Regarding a generic k-th target in the a-th acquisition, a general transformation between the coordinates referring to $o_P x_P y_P z_P$ (i.e., $[x_{P,k}, y_{P,k}, z_{P,k}]^T$) and those referring to $OXYZ$ (i.e., $[X_{k(a)}, Y_{k(a)}, Z_{k(a)}]^T$) is:

$$
\begin{bmatrix} X_{k(a)} \\ Y_{k(a)} \\ Z_{k(a)} \end{bmatrix} = \boldsymbol{R_{P(a)}} \cdot \begin{bmatrix} x_{P,k} \\ y_{P,k} \\ z_{P,k} \end{bmatrix} + \begin{bmatrix} X_{P(a)} \\ Y_{P(a)} \\ Z_{P(a)} \end{bmatrix},
\tag{18}
$$

where

$\boldsymbol{R_{P(a)}}$ is a rotation matrix, which depicts the probe orientation with respect to $OXYZ$, in the a-th acquisition. The elements of this matrix are functions of three (unknown) rotation angles ($\Omega_{P(a)}$, $\Phi_{P(a)}$, and $K_{P(a)}$) that are related to the axes x_P, y_P, z_P; $[X_{P(a)}, Y_{P(a)}, Z_{P(a)}]^T$ are the coordinates of P in $OXYZ$.
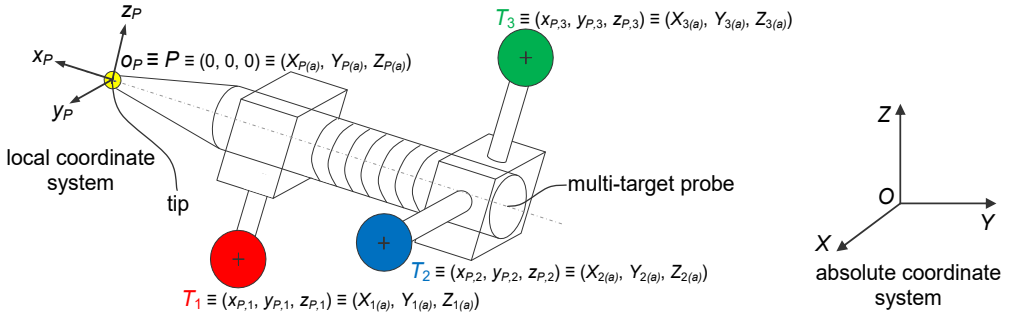
Fig. A.3. Local coordinate system of the multi-target probe ($o_Px_Py_Pz_P$) and the absolute coordinate system ($OXYZ$). The points corresponding to the probe tip and targets are expressed with respect to both systems.

Since the probe geometry is known (with some uncertainty), for each k-th target, we can define a position vector ($x_{P,k}$, $y_{P,k}$, $z_{P,k}$) referring to the local coordinate system $o_Px_Py_Pz_P$. The coordinates $x_{P,k}$, $y_{P,k}$, $z_{P,k}$ can be treated as random variables, whose dispersion depends on the precision with which the probe geometry was calibrated. Obviously, these coordinates are independent from the specific position/orientation of the probe (and therefore on the a-th acquisition) but they depend exclusively on the probe geometry. On the other hand, Eq. 18 includes six (unknown) parameters describing the specific position and orientation of the probe during the a-th acquisition: $X_{P(a)}$, $Y_{P(a)}$, $Z_{P(a)}$, $\Omega_{P(a)}$, $\Phi_{P(a)}$, $K_{P(a)}$.

Combining the transformations in Eqs. 12 and 18, we obtain the following equation for the sensors of type-A instruments:

$$\begin{bmatrix} x_{i.j,k(a)} \\ y_{i.j,k(a)} \\ z_{i.j,k(a)} \end{bmatrix} = \boldsymbol{R}_{i.j}^{T} \left\{ \boldsymbol{R}_{P(a)} \cdot \begin{bmatrix} x_{P,k} \\ y_{P,k} \\ z_{P,k} \end{bmatrix} + \begin{bmatrix} X_{P(a)} \\ Y_{P(a)} \\ Z_{P(a)} \end{bmatrix} - \begin{bmatrix} X_{0_{i.j}} \\ Y_{0_{i.j}} \\ Z_{0_{i.j}} \end{bmatrix} \right\}. \tag{19}$$

Combining the transformations in Eqs. 17 and 18, the following equation can be obtained for the sensors of type-B instruments:

$$\begin{bmatrix} x_{i.j,k(a)} \\ y_{i.j,k(a)} \\ z_{i.j,k(a)} \end{bmatrix} = \boldsymbol{r}_{i.j}^{T} \cdot \left(\boldsymbol{R}_{i.\bullet}^{T} \cdot \left\{ \boldsymbol{R}_{P(a)} \cdot \begin{bmatrix} x_{P,k} \\ y_{P,k} \\ z_{P,k} \end{bmatrix} + \begin{bmatrix} X_{P(a)} \\ Y_{P(a)} \\ Z_{P(a)} \end{bmatrix} - \begin{bmatrix} X_{0_{i.\bullet}} \\ Y_{0_{i.\bullet}} \\ Z_{0_{i.\bullet}} \end{bmatrix} \right\} - \begin{bmatrix} x_{0_{i.j}} \\ y_{0_{i.j}} \\ z_{0_{i.j}} \end{bmatrix} \right). \tag{20}$$

The relationships in Eqs. 19 and 20 will be used to express the coordinates of a target $(x_{i.j,k(a)}, y_{i.j,k(a)}, z_{i.j,k(a)})$, referring to the relevant sensor's local coordinate system, as functions of the unknowns of the problem. It can be noted that Eq. 19 can be interpreted as a specific case of (the more general) Eq. 20, in which the local coordinate systems $o_{i.\bullet}x_{i.\bullet}y_{i.\bullet}z_{i.\bullet}$ and $o_{i.j}x_{i.j}y_{i.j}z_{i.j}$ coincide, matrices $\boldsymbol{R}_{i.\bullet}$ and $\boldsymbol{R}_{i.j}$ coincide, and $\boldsymbol{r}_{i.j}$ is an identity matrix.

A.2.3 Local coordinate system related to the probe integrated sensors

The integrated (inertial) sensors of the probe perform angular measurements referring to an absolute ground-referenced coordinate system with (i) arbitrary origin, (ii) Z axis coinciding with the normal vector to the ground plane, and (iii) X axis pointing toward the magnetic north. The orientation of the absolute coordinate system ($OXYZ$) is conventionally coincident with that of this one.

During each a-th acquisition, the integrated sensors provide an estimate of the unknown rotation angles of the probe ($\hat{\Omega}_{P(a)}, \hat{\Phi}_{P(a)}, \hat{K}_{P(a)}$), with respect to $OXYZ$.

A.3 Details on equation formulation

This section describes in detail the formulation of equations for the global calibration problem, distinguishing between equations for distance, angular sensors, integrated probe sensors and additional artefacts.

A.3.1 Distance sensors

Considering the local perspective of a generic *i.j*-th distance sensor and for a generic *a*-th acquisition, the distance between the *k*-th target and the origin of the local coordinate system $o_{i,j}x_{i,j}y_{i,j}z_{i,j}$ – can be calculated as (see Fig. A.1):

$$d_{i.j,k(a)} = \sqrt{x_{i.j,k(a)}^2 + y_{i.j,k(a)}^2 + z_{i.j,k(a)}^2} \; . \qquad (21)$$

Eq. 21 can be reformulated as a function of the unknown variables of the problem, which are contained in the column vector X (in Eq. 1), applying the transformations in Eqs. 19 (for type-A instruments) or 20 (for type-B instruments). Of course, the resulting equation will not be linear with respect to X.

Among the unknowns in X, it can be demonstrated that only those relating to the absolute position (not the orientation) of distance sensors appear in Eqs. 19 and 20. In fact, distance sensors can be seen as special punctiform sensors, whose orientation is arbitrary; the unknown orientation angles could therefore be omitted from the unknowns of the problem (or replaced with arbitrary numerical values).

A linearization of the above equation can be obtained through a Taylor expansion with respect to the parameters in X.

The resulting linearized equation – which is related to the *i.j*-th distance sensor and *k*-th target, in the *a*-th acquisition – can be expressed in matrix form as:

$$A_{i.j,k(a)}^{dist} \cdot X - B_{i.j,k(a)}^{dist} = 0 , \qquad (22)$$

where X is the (unknown) vector (see Eq. 1) and matrices $A_{i.j,k(a)}^{dist}$ and $B_{i.j,k(a)}^{dist}$ contain (demonstration omitted):

- the distance $d_{i.j,k(a)}$;
- information on the geometry of the probe and that of the relevant instrument (for type-B instruments only);

- some initial values ($\hat{\hat{X}}^{(1)}$) related to the unknown variables.

A.3.2 Angular sensors

Considering the local perspective of a generic *i.j*-th angular sensor, the line passing through the *k*-th target (T_k) and $o_{i,j}$ (see Fig. A.1) subtends two angles – i.e., $\theta_{i,j,k(a)}$ (azimuth) and $\varphi_{i,j,k(a)}$ (elevation). Precisely, $\theta_{i,j,k(a)}$ describes the inclination of segment $o_{i,j}T_k$ with respect to the plane $x_{i,j}y_{i,j}$ (with a positive sign when $z_{i,j} > 0$), while $\varphi_{i,j,k(a)}$ describes the counterclockwise rotation of the projection ($o_{i,j}T_k{}'$) of $o_{i,j}T_k$ on the $x_{i,j}y_{i,j}$ plane, with respect to the $x_{i,j}$ axis. Subscript "(*a*)" indicates that the above angles may change from acquisition to acquisition. The following relationships can be expressed considering to the local coordinate system of the *i.j*-th sensor:

$$\theta_{i.j,k(a)} = \tan^{-1}\frac{y_{i.j,k(a)}}{x_{i.j,k(a)}} \qquad \begin{cases} \text{if } x_{i.j,k(a)} \geq 0 \text{ then } -\frac{\pi}{2} \leq \theta_{i.j,k(a)} \leq \frac{\pi}{2} \\ \text{if } x_{i.j,k(a)} < 0 \text{ then } \frac{\pi}{2} < \theta_{i.j,k(a)} < \frac{3\pi}{2} \end{cases} \tag{23}$$

$$\varphi_{i.j,k(a)} = \sin^{-1}\frac{z_{i.j,k(a)}}{o_{i.j}T_k} \qquad \left\{ -\frac{\pi}{2} \leq \varphi_{i.j,k(a)} \leq \frac{\pi}{2} \right.$$

Given that:

$$\tan\theta_{i.j,k(a)} = \frac{\sin\theta_{i.j,k(a)}}{\cos\theta_{i.j,k(a)}} \tag{24}$$

and

$$o_{i.j}T_k = \frac{o_{i.j}T_k{}'}{\cos\varphi_{i.j,k(a)}} = \frac{x_{i.j,k(a)}/\cos\theta_{i.j,k(a)}}{\cos\varphi_{i.j,k(a)}} = \frac{x_{i.j,k(a)}}{\cos\theta_{i.j,k(a)}\cdot\cos\varphi_{i.j,k(a)}}, \tag{25}$$

Eq. 23 can be reformulated as:

---

[1] The "double-hat" symbol "$\hat{\hat{}}$" indicates that a vector "close" to X can be obtained through a rough estimate of $\hat{X}$, i.e., the (final) estimate of X itself. We will illustrate how to determine $\hat{X}$ later.

$$\begin{cases} x_{i.j,k(a)} \cdot \sin\theta_{i.j,k(a)} - y_{i.j,k(a)} \cdot \cos\theta_{i.j,k(a)} = 0 \\ x_{i.j,k(a)} \cdot \sin\varphi_{i.j,k(a)} - z_{i.j,k(a)} \cdot \cos\theta_{i.j,k(a)} \cdot \cos\varphi_{i.j,k(a)} = 0 \end{cases}. \tag{26}$$

The system in Eq. 26 can be reformulated as a function of the unknowns of the problem, applying the transformation in Eq. 19, for network sensors of type-A instruments with unknown geometry, or Eq. 20 for network sensors of type-B instruments. Of course, the resulting equations will not be linear with respect to the unknown variables in X. However, a linearization can be obtained through a Taylor expansion with respect to the parameters contained in X, considering some $\hat{X}$ values reasonably close to them. This operation can be automated through the Matlab's function "functionalDerivative" or other symbolic-calculation tools.

The resulting linearized equations can be expressed in matrix form as:

$$A_{i.j,k(a)}^{ang} \cdot X - B_{i.j,k(a)}^{ang} = 0, \tag{27}$$

where X is the (unknown) vector (see Eq. 1) and matrices $A_{i.j,k(a)}^{ang}$ and $B_{i.j,k(a)}^{ang}$ contain (demonstration omitted):

- the angles $\theta_{i.j,k(a)}$ and $\varphi_{i.j,k(a)}$;
- information on the geometry of the probe and that of the sensor's instrument (for type-B instruments only);
- some initial values ($\hat{X}$) related to the unknown variables in X.

A.3.3 Integrated sensors of the probe

The integrated (inertial) probe sensors may contribute to estimate the probe orientation angles, for a generic a-th acquisition. The fact that angular measurements are related to a ground-referenced coordinate system oriented according to $OXYZ$ entails that they can be directly used as estimates of the probe orientation angles $\hat{\Omega}_{P(a)}, \hat{\Phi}_{P(a)}, \hat{K}_{P(a)}$. For a generic a-th acquisition, three (relatively trivial) equations are therefore available:

$$\hat{\Omega}_{P(a)} = \Omega_{P(a)}$$
$$\hat{\Phi}_{P(a)} = \Phi_{P(a)} \; .$$
$$\hat{K}_{P(a)} = K_{P(a)}$$

(28)

These (linear) equations can be expressed in matrix form as:

$$A_{(a)}^{int} \cdot X - B_{(a)}^{int} = 0 \; .$$

(29)

We remark that the uncertainty in the angular measurements of the integrated sensors depends on their technological characteristics, although it is likely to be higher than those in the local measurements by network sensors. These aspects will be taken into account in the weighing phase of the equations (see Sects. 2.3 and A.4).

A.3.4 Additional artefact

The use of additional artefact(s) where to position the probe tip during acquisitions allows to formulate other equations for the problem of interest. Precisely, an additional artefact may have a number of reference points (e.g., four, *A*, *B*, *C* and *D*, as exemplified in Sect. 3). The probe acquisitions can be subdivided into "clusters" (*c* = 1, 2, ...), in which the artefact has a fixed position, and the probe is positioned in the various reference points, acquisition by acquisition. For example, when using an artefact with four reference points, each cluster will include four acquisitions, in which the artefact has a fixed position, and the probe is repositioned in each of the four reference points respectively.

Since the geometry of the additional artefact is known in terms of mutual distances between the reference points (e.g., they can be determined through an *ad hoc* geometric calibration, e.g., using a CMM), it is possible to formulate additional equations. Specifically, an Euclidean distance equation can be formulated for each of the pairs (*a'* e *a''*) of acquisitions of a certain *c*-th cluster, resulting from the (non-reflective and symmetric) Cartesian product A_c x A_c, being A_c the set of acquisitions in the *c*-th cluster:

$$d_{(a',a'')_c} = \sqrt{\left(X_{P(a')_c} - X_{P(a'')_c}\right)^2 + \left(Y_{P(a')_c} - Y_{P(a'')_c}\right)^2 + \left(Z_{P(a')_c} - Z_{P(a'')_c}\right)^2} \; ,$$

(30)

where $d_{(a',a'')_c}$ corresponds to a known distance – since it can be estimated in a previous geometric-calibration process of the additional artefact. Obviously, this equation is not linear with respect to the output variables (i.e., $X_{P(a')_c}$, $Y_{P(a')_c}$, $Z_{P(a')_c}$, $X_{P(a'')_c}$, $Y_{P(a'')_c}$, $Z_{P(a'')_c}$). A linearization can be obtained through a first order Taylor expansion with respect to these variables. The resulting linearized equations can be expressed in matrix form as:

$$A^{art}_{(a',a'')_c} \cdot X - B^{art}_{(a',a'')_c} = 0, \tag{31}$$

where matrices $A^{art}_{(a',a'')_c}$ and $B^{art}_{(a',a'')_c}$ contain initial values of the unknown coordinates of the probe tip and the known (albeit with some uncertainty) distance $d_{(a',a'')_c}$ (demonstration omitted). Since this equation contains previously estimated distance parameters, it contributes to metrological traceability with respect to the measurement unit of length.

A.4 Note on matrices J and Σ_ξ

This section goes deeper into what is described in Sect. 2.3, regarding the weighing of the system in Eq. 2.

Focusing on the second member of Eq. 5, J is the Jacobian matrix with the partial derivatives of the elements in the first members of Eq. 2 with respect to the elements in ξ (Eq. 4)

$$J = \begin{bmatrix} J^{probe} & 0 & 0 & 0 & 0 \\ 0 & J^{type-B\ instr.} & 0 & 0 & 0 \\ 0 & 0 & J^{add.artef.} & 0 & 0 \\ 0 & 0 & 0 & J^{network\ sens.} & 0 \\ 0 & 0 & 0 & 0 & J^{integr.\ sens.} \end{bmatrix}. \tag{32}$$

where,
$$J^{probe} = \begin{bmatrix} \ddots & & 0 \\ & J_k^{probe} & \\ 0 & & \ddots \end{bmatrix}, \qquad J^{type-B\ instr.} = \begin{bmatrix} \ddots & & 0 \\ & J_{i.j}^{type-B\ instr.} & \\ 0 & & \ddots \end{bmatrix},$$

$$J^{add.artef.} = \begin{bmatrix} \ddots & & 0 \\ & J_{(a',a'')_c}^{add.artef.} & \\ 0 & & \ddots \end{bmatrix}, \qquad J^{network\ sens.} = \begin{bmatrix} \ddots & & 0 \\ & J_{i.j,k(a)}^{network\ sens.} & \\ 0 & & \ddots \end{bmatrix},$$

$$J^{integr.\ sens.} = \begin{bmatrix} \ddots & & 0 \\ & J_{(a)}^{integr.\ sens.} & \\ 0 & & \ddots \end{bmatrix}.$$

In general, J^* is a Jacobian (block-diagonal) matrix containing the partial derivatives related to the elements in the sub-vector ξ^*. The calculation of such derivatives can be automated through the Matlab's symbolic-calculation function "functionalDerivative" or other symbolic-calculation tools.

Returning to the second member of Eq. 5, Σ_ξ is the covariance matrix of ξ:

$$\Sigma_\xi = \begin{bmatrix} \Sigma_\xi^{probe} & 0 & 0 & 0 & 0 \\ 0 & \Sigma_\xi^{type-B\ instr.} & 0 & 0 & 0 \\ 0 & 0 & \Sigma_\xi^{add.artef.} & 0 & 0 \\ 0 & 0 & 0 & \Sigma_\xi^{network\ sens.} & 0 \\ 0 & 0 & 0 & 0 & \Sigma_\xi^{integr.\ sens.} \end{bmatrix}, \qquad (33)$$

where
$$\Sigma_\xi^{probe} = \begin{bmatrix} \ddots & & 0 \\ & \Sigma_{\xi k}^{probe} & \\ 0 & & \ddots \end{bmatrix}, \qquad \Sigma_\xi^{type-B\ instr.} = \begin{bmatrix} \ddots & & 0 \\ & \Sigma_{\xi i.j}^{type-B\ instr.} & \\ 0 & & \ddots \end{bmatrix},$$

$$\Sigma_\xi^{add.artef.} = \begin{bmatrix} \ddots & & 0 \\ & \Sigma_{\xi(a)}^{add.artef.} & \\ 0 & & \ddots \end{bmatrix}, \qquad \Sigma_\xi^{network\ sens.} = \begin{bmatrix} \ddots & & 0 \\ & \Sigma_{\xi i.j,k(a)}^{network\ sens.} & \\ 0 & & \ddots \end{bmatrix},$$

$$\Sigma_\xi^{integr.sens.} = \begin{bmatrix} \ddots & & 0 \\ & \Sigma_{\xi(a)}^{integr.sens.} & \\ 0 & & \ddots \end{bmatrix}. \qquad (34)$$

Σ_ξ can be split into sub-block matrices Σ_ξ^*, which can be interpreted as the covariance matrices of the ξ^* sub-vectors.

While the (co)variances concerned with (i) type-B LVM instruments (in $\Sigma_\xi^{type\text{-}B\ instr.}$), (ii) probe targets (in Σ_ξ^{probe}) and (iii) additional artefact (in $\Sigma_\xi^{add.artefact}$) can be obtained from preliminary *ad hoc* geometric calibration process(es), those concerned with (iv) the angular/distance measurements by network sensors (in $\Sigma_\xi^{network\ sens.}$) and (v) probe's inertial sensors ($\Sigma_\xi^{integr.sens.}$) can be determined from manuals and technical documents relating to the sensors in use, or estimated through *ad hoc* experimental tests.

The off-diagonal entries in the (sub-)blocks are zeros, assuming no correlation between these parameters [10].

A.5 Further study on uncertainty estimation

This section provides additional information on the construction of the covariance matrix Σ_X (see Eq. 7), which is used for estimating the uncertainty in the location of network sensors.

The most interesting parts of the above matrix are the 6x6 blocks depicting the variability in the estimates of the position/orientation of each type-B instrument or network sensor of a type-A instruments (i.e., the sub-blocks related to $X_{i.j}^{type-A\ instr.}$ and $X_{i.\bullet}^{type-B\ instr.}$, as shown in Eq. 35.

$$\Sigma_{X_{i.j}^{type-A\ instr.}} = \begin{bmatrix}
\hat{\sigma}^2_{X_{0i.j}} & \hat{\sigma}_{X_{0i.j}}\hat{\sigma}_{Y_{0i.j}} & \hat{\sigma}_{X_{0i.j}}\hat{\sigma}_{Z_{0i.j}} & \hat{\sigma}_{X_{0i.j}}\hat{\sigma}_{\Omega_{i.j}} & \hat{\sigma}_{X_{0i.j}}\hat{\sigma}_{\Phi_{i.j}} & \hat{\sigma}_{X_{0i.j}}\hat{\sigma}_{K_{i.j}} \\
\hat{\sigma}_{X_{0i.j}}\hat{\sigma}_{Y_{0i.j}} & \hat{\sigma}^2_{Y_{0i.j}} & \hat{\sigma}_{Y_{0i.j}}\hat{\sigma}_{Z_{0i.j}} & \hat{\sigma}_{Y_{0i.j}}\hat{\sigma}_{\Omega_{i.j}} & \hat{\sigma}_{Y_{0i.j}}\hat{\sigma}_{\Phi_{i.j}} & \hat{\sigma}_{Y_{0i.j}}\hat{\sigma}_{K_{i.j}} \\
\hat{\sigma}_{X_{0i.j}}\hat{\sigma}_{Z_{0i.j}} & \hat{\sigma}_{Y_{0i.j}}\hat{\sigma}_{Z_{0i.j}} & \hat{\sigma}^2_{Z_{0i.j}} & \hat{\sigma}_{Z_{0i.j}}\hat{\sigma}_{\Omega_{i.j}} & \hat{\sigma}_{Z_{0i.j}}\hat{\sigma}_{\Phi_{i.j}} & \hat{\sigma}_{Z_{0i.j}}\hat{\sigma}_{K_{i.j}} \\
\hat{\sigma}_{X_{0i.j}}\hat{\sigma}_{\Omega_{i.j}} & \hat{\sigma}_{Y_{0i.j}}\hat{\sigma}_{\Omega_{i.j}} & \hat{\sigma}_{Z_{0i.j}}\hat{\sigma}_{\Omega_{i.j}} & \hat{\sigma}^2_{\Omega_{i.j}} & \hat{\sigma}_{\Omega_{i.j}}\hat{\sigma}_{\Phi_{i.j}} & \hat{\sigma}_{\Omega_{i.j}}\hat{\sigma}_{K_{i.j}} \\
\hat{\sigma}_{X_{0i.j}}\hat{\sigma}_{\Phi_{i.j}} & \hat{\sigma}_{Y_{0i.j}}\hat{\sigma}_{\Phi_{i.j}} & \hat{\sigma}_{Z_{0i.j}}\hat{\sigma}_{\Phi_{i.j}} & \hat{\sigma}_{\Omega_{i.j}}\hat{\sigma}_{\Phi_{i.j}} & \hat{\sigma}^2_{\Phi_{i.j}} & \hat{\sigma}_{\Phi_{i.j}}\hat{\sigma}_{K_{i.j}} \\
\hat{\sigma}_{X_{0i.j}}\hat{\sigma}_{K_{i.j}} & \hat{\sigma}_{Y_{0i.j}}\hat{\sigma}_{K_{i.j}} & \hat{\sigma}_{Z_{0i.j}}\hat{\sigma}_{K_{i.j}} & \hat{\sigma}_{\Omega_{i.j}}\hat{\sigma}_{K_{i.j}} & \hat{\sigma}_{\Phi_{i.j}}\hat{\sigma}_{K_{i.j}} & \hat{\sigma}^2_{K_{i.j}}
\end{bmatrix} ,$$

$$\Sigma_{X_{i.\bullet}^{type-B\ instr.}} = \begin{bmatrix}
\hat{\sigma}^2_{X_{0i.\bullet}} & \hat{\sigma}_{X_{0i.\bullet}}\hat{\sigma}_{Y_{0i.\bullet}} & \hat{\sigma}_{X_{0i.\bullet}}\hat{\sigma}_{Z_{0i.\bullet}} & \hat{\sigma}_{X_{0i.\bullet}}\hat{\sigma}_{\Omega_{i.\bullet}} & \hat{\sigma}_{X_{0i.\bullet}}\hat{\sigma}_{\Phi_{i.\bullet}} & \hat{\sigma}_{X_{0i.\bullet}}\hat{\sigma}_{K_{i.\bullet}} \\
\hat{\sigma}_{X_{0i.\bullet}}\hat{\sigma}_{Y_{0i.\bullet}} & \hat{\sigma}^2_{Y_{0i.\bullet}} & \hat{\sigma}_{Y_{0i.\bullet}}\hat{\sigma}_{Z_{0i.\bullet}} & \hat{\sigma}_{Y_{0i.\bullet}}\hat{\sigma}_{\Omega_{i.\bullet}} & \hat{\sigma}_{Y_{0i.\bullet}}\hat{\sigma}_{\Phi_{i.\bullet}} & \hat{\sigma}_{Y_{0i.\bullet}}\hat{\sigma}_{K_{i.\bullet}} \\
\hat{\sigma}_{X_{0i.\bullet}}\hat{\sigma}_{Z_{0i.\bullet}} & \hat{\sigma}_{Y_{0i.\bullet}}\hat{\sigma}_{Z_{0i.\bullet}} & \hat{\sigma}^2_{Z_{0i.\bullet}} & \hat{\sigma}_{Z_{0i.\bullet}}\hat{\sigma}_{\Omega_{i.\bullet}} & \hat{\sigma}_{Z_{0i.\bullet}}\hat{\sigma}_{\Phi_{i.\bullet}} & \hat{\sigma}_{Z_{0i.\bullet}}\hat{\sigma}_{i.\bullet} \\
\hat{\sigma}_{X_{0i.\bullet}}\hat{\sigma}_{\Omega_{i.\bullet}} & \hat{\sigma}_{Y_{0i.\bullet}}\hat{\sigma}_{\Omega_{i.\bullet}} & \hat{\sigma}_{Z_{0i.\bullet}}\hat{\sigma}_{\Omega_{i.\bullet}} & \hat{\sigma}^2_{\Omega_{i.\bullet}} & \hat{\sigma}_{\Omega_{i.\bullet}}\hat{\sigma}_{\Phi_{i.\bullet}} & \hat{\sigma}_{\Omega_{i.\bullet}}\hat{\sigma}_{K_{i.\bullet}} \\
\hat{\sigma}_{X_{0i.\bullet}}\hat{\sigma}_{\Phi_{i.\bullet}} & \hat{\sigma}_{Y_{0i.\bullet}}\hat{\sigma}_{\Phi_{i.\bullet}} & \hat{\sigma}_{Z_{0i.\bullet}}\hat{\sigma}_{\Phi_{i.\bullet}} & \hat{\sigma}_{\Omega_{i.\bullet}}\hat{\sigma}_{\Phi_{i.\bullet}} & \hat{\sigma}^2_{\Phi_{i.\bullet}} & \hat{\sigma}_{\Phi_{i.\bullet}}\hat{\sigma}_{K_{i.\bullet}} \\
\hat{\sigma}_{X_{0i.\bullet}}\hat{\sigma}_{K_{i.\bullet}} & \hat{\sigma}_{Y_{0i.\bullet}}\hat{\sigma}_{K_{i.\bullet}} & \hat{\sigma}_{Z_{i.\bullet}}\hat{\sigma}_{K_{i.\bullet}} & \hat{\sigma}_{\Omega_{i.\bullet}}\hat{\sigma}_{K_{i.\bullet}} & \hat{\sigma}_{\Phi_{i.\bullet}}\hat{\sigma}_{K_{i.\bullet}} & \hat{\sigma}^2_{K_{i.\bullet}}
\end{bmatrix}$$

(35)

For a generic $i.j$-th type-A sensor, we can use the diagonal elements of the top-left 3x3 sub-block of $\Sigma_{X_{i.j}^{type-A\,instr.}}$, to calculate the *expanded uncertainties* associated with the position Cartesian coordinates:

$$
\begin{aligned}
U_{X_{0_{i.j}}} &= k \cdot \hat{\sigma}_{X_{i.j}} \\
U_{Y_{0_{i.j}}} &= k \cdot \hat{\sigma}_{Y_{i.j}} \quad , \\
U_{Z_{0_{i.j}}} &= k \cdot \hat{\sigma}_{Z_{i.j}}
\end{aligned}
\tag{36}
$$

where $k = 2$ is the so-called *coverage factor*, which means that – for normally distributed estimates of $X_{0_{i.j}}$, $Y_{0_{i.j}}$, $Z_{0_{i.j}}$ – the corresponding coverage probability is 95% (JCGM 100:2008, 2008).

An estimate of the expanded uncertainty related to the sensor position can be obtained through the sum of squared uncertainties in Eq. 36:

$$
U_{0_{i.j}} = \sqrt{U_{X_{0_{i.j}}}^2 + U_{Y_{0_{i.j}}}^2 + U_{X_{0_{i.j}}}^2} = k \cdot \sqrt{\hat{\sigma}_{X_{i.j}}^2 + \hat{\sigma}_{Y_{i.j}}^2 + \hat{\sigma}_{Z_{i.j}}^2} \quad ,
\tag{37}
$$

Similarly, for a generic $i.\bullet$-th type-B instrument, we obtain:

$$
U_{0_{i.\bullet}} = \sqrt{U_{X_{0_{i.\bullet}}}^2 + U_{Y_{0_{i.\bullet}}}^2 + U_{X_{0_{i.\bullet}}}^2} = k \cdot \sqrt{\hat{\sigma}_{X_{i.\bullet}}^2 + \hat{\sigma}_{Y_{i.\bullet}}^2 + \hat{\sigma}_{Z_{i.\bullet}}^2} \quad .
\tag{38}
$$

An estimate of the expanded uncertainty associated with the probe position in a generic a-th acquisition can be obtained following an analogous reasoning, resulting in:

$$
U_{P(a)} = \sqrt{U_{X_{P(a)}}^2 + U_{Y_{P(a)}}^2 + U_{X_{P(a)}}^2} = k \cdot \sqrt{\hat{\sigma}_{X_{P(a)}}^2 + \hat{\sigma}_{Y_{P(a)}}^2 + \hat{\sigma}_{Z_{P(a)}}^2} \quad .
\tag{39}
$$